AN IMPROVED APPROACH FOR SOIL MOISTURE ESTIMATION BY EMPLOYING ILLUMINATION-CORRECTED DATA IN A MODIFIED T_s-VI METHOD

AMER ABDALLA AHMAD

September 2011

TECHNICAL REPORT
NO. 277

AN IMPROVED APPROACH FOR SOIL MOISTURE ESTIMATION BY EMPLOYING ILLUMINATION-CORRECTED DATA IN A MODIFIED T_S-VI METHOD

Amer Abdalla Ahmad

Department of Geodesy and Geomatics Engineering
University of New Brunswick
P.O. Box 4400
Fredericton, N.B.
Canada
E3B 5A3

September, 2011

PREFACE

This technical report is a reproduction of a thesis submitted in partial fulfillment of the requirements for the degree of Master of Science in Engineering in the Department of Geodesy and Geomatics Engineering, September 2011. The research was supervised by Dr. Yun Zhang, and support was provided by the Government of Iraq. As with any copyrighted material, permission to reprint or quote extensively from this report must be received from the author. The citation to this work should appear as follows:

Ahmad, Amer (2011). *An Improved Approach For Soil Moisture Estimation By Employing Illumination-Corrected Data in a Modified T_s-VI Method* . M.Sc.E. thesis, Department of Geodesy and Geomatics Engineering Technical Report No. 277, University of New Brunswick, Fredericton, New Brunswick, Canada, 112 pp.

DEDICATION

This thesis is dedicated to my closest person, my dear friend, my idol, and my great mother. I am deeply and forever indebted to you for your love, support and encouragement throughout my entire life.

ABSTRACT

There are a great number of publications that apply different methods to estimate soil moisture from optical satellite imagery. However, none of the proposed methods have considered correcting solar illumination error that is caused by variation in topography before estimating soil moisture.

In this research, an integrated approach is developed to improve the estimation of soil moisture. The integration is represented by removing the solar-illumination error from the data. Several modifications were made in the T_s-VI space based on the Universal Triangle Relationship. The data used in the research are obtained from Moderate Resolution Imaging Spectroradiometer (MODIS) satellite.

The research results show that the surface-illumination error, which is caused by variation in topography, misleads the estimation of soil moisture index. Based on statistical and visual analysis, the results are improved with removing error. The method is further enhanced with the application of enhanced vegetation index (EVI) to the T_s-VI relationship.

ACKNOWLEDGEMENTS

I would primarily like to thank Dr. Yun Zhang and Dr. Sue Nichols for their continuous support and providing me with the opportunity to conduct this research. Without their support, this research would not have been possible. In addition, I would like to express on my sincere gratitude to Dr. Yun Zhang for the time that he spent in reviewing my papers, supervising and providing me with proper guidance to complete the research. Thanks to Dr. Darka Mioc for her continuous support and guidance, in particular, when she was my co-advisor. I would like to thank both Dr. Charles Bourque and Dr. Fan-Rui Meng for their constructive comments and continuous support during my research.

I would like to thank the Iraqi Ministry of Higher Education for providing me with financial support during my study.

Thanks are given to the staff at the GGE Department and to my colleagues that were around me at UNB. The study environment and supporting staff was excellent and I will cherish the friendships I have made in this faculty for a long time.

I also would like to thank my mother, brothers and other close friends back home for their encouragement and support from abroad during my study. Their support was essential in tough times. Last, but not least, I would like to thank my friends that were around me in Fredericton; we experienced highs and lows together and all the time that we have spent together will always be memorable.

TABLE OF CONTENTS

LIST OF TABLES

LIST OF FIGURES

LIST OF SYMBOLS AND ABBREVIATIONS

TVDI	Temperature Vegetation Dryness Index
EVI	Enhanced Vegetation Index
NDVI	Normalized Difference Vegetation Index
SR	Surface Reflectance
T_s	Land Surface Temperature
CR	Correlation Coefficient
μ	Mean
σ	Standard Deviation
VI	Vegetation Index
RMSE	Root Mean Square Error
GSM	Ground Soil Moisture
T_B	Brightness Temperature
DN	Digital Number
MODIS	Moderate Resolution Imaging Spectroradiometer
ET	Evapotranspiration
LIDAR	Light Detection And Ranging

CHAPTER 1

INTRODUCTION

This research presents a new approach to soil moisture estimation. The approach is based on correcting the data for solar-illumination effects and employing the corrected data in a modified Universal Triangle Relationship Method. The body of this work is presented through the following papers composing the thesis:

Paper 1 (peer reviewed):

Ahmad, A., Y. Zhang, and S. Nichols (2011). "Review and evaluation of remote sensing methods for soil-moisture estimation." *SPIE Reviews journal*, Vol.2, pp. 028001 1-17.

Paper 2:

Ahmad, A., and Y. Zhang (2011). "Development and challenges of applying the Universal Traingle relationship Method in remote sensing applications." *Proceedings of the 32nd Canadian Symposium on Remote Sensing and 14th Congress of the AQT*, Sherbrooke, Québec, Canada, June, 13-16, 2011.

Paper 3 (peer reviewed):

Ahmad, A., Y. Zhang, and C. Bourque (2011). "Mapping an Index of Soil-Moisture Using Illumination-Corrected Land Surface Temperature and Enhanced Vegetation Index Generated from MODIS Data." Will be submitted to the *Journal Remote Sensing of Environment*.

This chapter will present an introduction and an overview by composing the above three publications including the following sections:

1.1 An outline of the structure of this article-based thesis;

1.2 A background of soil moisture and environment;

1.3 Soil moisture estimation developments in remote sensing;

1.4 Problems of estimating soil moisture (Research Problem);

1.5 Research objectives;

1.6 Strategies to meet the objective; and

1.7 An overview of each chapter presented in this thesis.

1.1 Thesis Structure

For all the publications presented in this thesis, the first author conducted the primary research while the other authors provided the advice regarding revision of the structure and the contents; except for the last publication that was produced as a result of a group research work that was done by the authors and integrated in the form of a paper by the first author, Darka Mioc. The structure of the thesis is presented in Figure 1.1 below.

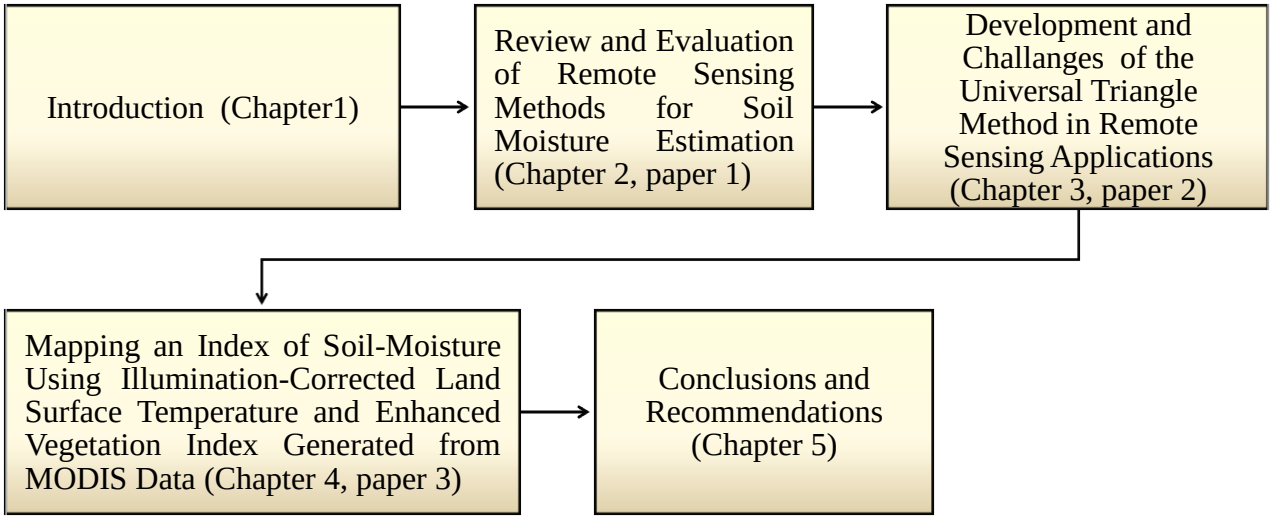

Figure 1.1 Thesis structure

1.2 Background of Soil Moisture and Environment

Soil moisture can be defined by the amount of water that the soil can hold for a period of time after precipitation. This amount of water varies depending on the soil characteristics and environmental conditions. This water contributes to the soil water content, is expressed quantitatively as a percentage from 0% (which is completely dry soil) to 100% (which is completely wet). The unit measurement for soil water content can be expressed as either a volumetric unit (θ_v) or a gravimetric unit (θ_g). A volumetric measurement usually refers to the quantitative amount of liquid water in the soil, which is

measured in m^3 of water/m^3 of soil. A gravimetric measurement is represented as a percentage of the weight of an amount of water in the soil divided by the weight of a mass of soil that retains it; therefore, its unit is in kg of water/ kg of dry soil [Nguyen, 2008].

Three main methods are used to measure soil water content: field measurements, laboratory measurements, and remote sensing. Each one of these methods has its own advantages and disadvantages depending on the procedure that is followed to measure the water content [Prichard, nd]. For instance, the volumetric method is normally applied in the field using different equipment (sensors) that are installed locally in a testing area; then the current conditions of the soil are measured within a short period of time. The other method is called the Gravimetric method; it tests the soil water content by taking a soil sample to the laboratory to be analyzed. The last method utilizes remote sensing technology and digital imagery; in this method, soil moisture is estimated from remotely acquired information

Surface soil moisture is defined as the amount of water available in the upper 10 cm of soil, whereas root zone soil moisture is the amount of water available to plants in the upper 200 cm of soil [James, 1999].

Soil moisture is strongly influenced by environmental conditions. These environmental conditions include precipitation, surface temperature, soil cover, and soil physical conditions such as texture, permeability, density, and soil composition. Many researchers have shown a negative correlation between soil moisture and mean and

maximum soil temperatures [Georgakakos et al., 1995; Huang et al., 1996]. Eltahir and Pal [1996] have established a relationship between soil moisture and rainfall; they have suggested that surface wet bulb temperature, which is an indication of surface conditions such as soil moisture, is positively correlated with convective rainfall amounts. Several studies focused on the role of soil moisture deficiency in causing droughts during the summer of 1988; most of these studies have focused on the relationship between increasing the circulation pattern of sea surface temperature and decreasing soil moisture [Trenberth et al., 1988]. Evaporation is another environmental factor that is impacted by soil moisture and as soil moisture increases, evaporation decreases accordingly especially during warm daytime temperatures [Owe et al., 2001; Yeh et al., 1984]. Up to now, soil cover has been recognized as a major factor that affects soil moisture conditions, but it has not been well investigated and accurately described by researchers.

In general, when an area experiences high precipitation and low surface temperature and low water drainage or when the area is covered with vegetation or snow, soil moisture is expected to increase and vice versa. Moreover, researchers try to discern the impact of soil water conditions on climate by using either numerical theoretical models or semi-empirical models, and relating these models' outcome results to the field soil moisture measurements. Several factors affect the soil moisture results from the currently used models reported by Haibin [2007]: precipitation forcing, radiation forcing, and the land surface. However, the lack of sufficient field soil measurements might affect the estimation results.

As a result, correct periodic monitoring for the changes in environmental conditions are necessary to avoid the unpredicted situations in the hydrological cycle and to determine soil moisture periodically as it changes over time.

1.3 Soil Moisture Estimation Development in Remote Sensing

After recognizing the need for an alternative solution to estimate the soil moisture remotely, major efforts were dedicated to initiate the concept of soil water estimation using remote sensing. In 1974, Schmugge et al. used the radiometer technique to estimate surface soil moisture. Later, Ulaby and Bush [1975] proposed using radar backscatter information to predict soil characteristics. Following that, Choudhury et al. [1979] and Schmugge [1980] published their first studies considering the effect of soil parameters such as soil roughness, soil texture, vegetation canopy, and surface temperature on estimated soil moisture. Jackson et al. [1981] were pioneers in introducing a direct approach to estimate soil moisture information using remote sensing data. Then, Dalal and Henry [1986] estimated soil moisture information with acceptable accuracy from a range of field soil samples, but they did not consider the effect of other soil parameters such as mineral soil composition, soil texture and soil organic matter. Until Jackson [1993] and Owe et al. [2001] initiated the first step to develop, refine, and validate regional and global soil moisture retrieval algorithms.

Currently, new approaches utilising different mathematical and theoretical models have been proposed and some of them have produced highly correlated results with the

in-situ measurements. For instance, neural networks and fuzzy logic algorithms have shown their effectiveness with passively and actively acquired remote sensing date [Ghedira et al., 2004; Said et al., 2008].

It has been noticed that each stage of development was commonly based: (i) the available remote sensing capability at that time; (ii) the effect of soil parameters that are considered in the study; and (iii) the data processing capability. On the other hand, different remote sensing spectral information can be utilized in different estimation methods. For instance, electromagnetic wavelength information, sources of electromagnetic energy, sensor configurations are all important factors play a role in obtaining better soil moisture estimation [Walker, 1999].

With the development of satellite imagery, new techniques to measure soil information have evolved. For instance, National Aeronautics and Space Administration (NASA) has played a crucial role in helping to develop different remote sensing applications by generously providing data online free of charge for research purposes.

Developing higher image spatial resolution and a uniform temporal resolution can allow better estimates of soil information within a few centimetres of the ground-space. But, the limitation of these estimated measurements will still lie in their inability to measure the water underneath a few centimetres of the soil surface. Even though new studies have been published to measure soil information at the root zone, none of these studies have been successful in measuring soil moisture accurately as compared with estimating soil moisture at the top centimetres of the soil.

With the current remote sensing technology, estimating soil moisture accurately enough to replace soil moisture field measurements is not possible

1.4 Research Problem

Optical imagery depends on the interaction of solar energy with the underlying terrain. This dependency makes the process of capturing satellite imagery vulnerable to variation in atmospheric and land surface conditions. This exposure to difference sun angles and variant satellite-topography angles causes surface illumination. Land-surface elements facing the sun appear bright and land-surface elements facing away from the sun appear dark, as a result of self-shading. With respect to soil water, these bright spots and dark spots cause misinterpretation whether these coloured spots are caused by the soil water characteristics or because of the sun-illumination.

Generally, bright spots in satellite imagery corresponding with flat terrain (assuming no change in satellite incidence angle) are likely to be classified as dry and hot. The situation, however, becomes considerably more complicated when dealing with areas in variable terrain. Variation in topography causes elements of the terrain (pixels) to have different orientations to the sun. Consequently, confusion might arise as to whether an area is illuminated because of its orientation to the sun or because of its inherent moisture status. Clearly, correct interpretation of a pixel's soil moisture status demands that terrain-induced illumination effects are removed prior estimating soil moisture.

1.5 Research Objective

The aim of this research is to improve the estimation of soil moisture from optical satellite imagery, in particular MODIS imagery. To meet this goal, a number of supporting tasks include:

a. Conducting a literature review of currently used methods in the estimation of soil moisture. Then, identifying the most widely used method;
b. Researching possible improvements in soil moisture estimation. This improvement can be achieved by integrating both illumination corrected data and improved estimation methodology; and
c. Studying the influential factors that degrade the pixel values in optical imagery; the factors that can mislead in the estimation of soil moisture.

The two main important aspects of improvement were (i) reducing the effect of variation in solar-illumination caused by variation in topography variations and (ii) applying modified parameters in the universal triangle method in estimating soil moisture

1.6 Proposed Methodology

This section outlines the research that will be performed to meet the outlined objectives. The data used in this research will be obtained from MODIS imagery, which are land surface temperature - emissivity (MOD11), surface reflectance (MOD09) from the Land Processes Distributed Active Archive Center together with MODIS Geolocation (MOD03) from the LAADS website (Level 1 and Atmosphere Archive and Distribution System; http://ladsweb.nascom.nasa.gov_). The data process will be implemented using MATLAB, ENVI, ERDAS and PCI software.

This thesis integrated approach was proposed after reviewing a wide range of methods to estimate soil moisture information (Chapter 2); this helped in identifying the most widely used method to estimate soil moisture information, which is the Universal Triangle Relationship Method. Then, research was conducted to find the key improvements for the easily implemented and widely used method, Universal Triangle Relationship Method that can lead to better soil moisture estimation (Chapter 3). Later, a new approach was developed to integrate illumination-corrected data in the modified Universal Triangle Relationship Method; then, the results were analyzed and discussed (Chapter 4).

The new integrated approach was developed using the most effective method in removing solar-illumination effect C-correction method. Then, the surface-illumination

removed data was employed in the modified universal triangle method to estimate soil moisture. The result analysis was implemented based on statistical and visual comparison before and after removing the solar-illumination. Conclusions and recommendations are drawn based on the outcome results (Chapter 5).

1.7 Overview of Each Chapter

This thesis is organized into five chapters. **Chapter One** sets the stage to an introduction to this thesis structure and to soil moisture relationship with environment, stage of soil moisture development in remote sensing. Then it summarizes the research problem, methodology and objective.

Chapter Two contains a review of methods using remote sensing data. Different methods are summarized, compared and ranked based on the best estimation results found in applying each method. It includes all the material that was published in the International Society for Optics and Photonics (SPIE) Reviews Journal on 28th February, 2011.

Chapter Three introduces the Modified Universal Triangle Method that was applied as part of the integrated approach to estimate soil moisture. The method's structure, development and challenges are discussed. A conclusion is drawn based on the statistical

and visual analysis and by comparing the estimation results with the maps of wetland. The material in this paper was presented and accepted for publication in the proceedings of the 32nd Canadian Symposium on Remote Sensing and 14th Congress of the AQT Conference, Sherbrooke, Québec, Canada on June 13th -16th , 2011.

Chapter Four presents the developed approach developed in this research. It discusses the integrated approach to correct the illumination error and then utilizes the corrected data to estimate soil moisture using a modified version of the universal triangle method. The research results are compared before and after the illumination correction, and before and after modifying the triangle method. A conclusion is drawn based on their comparisons. This chapter includes all the material that will be submitted to Remote Sensing of Environment.

Chapter Five concludes this research. It includes a conclusion and a recommendation drawn after the research approach was implemented and the results were analyzed. Possible future work is discussed to extend the work that was developed in this research.

References

Bush, T. F., and F. T. Ulaby (1975). "Fading characteristics of panchromatic radar backscatter from selected agricultural targets." *IEEE Transactions on Geoscience Electron,* Vol.GE-13, pp.149.

Choudhury, B. J., T. J. Schmugge, R. W. Newton , and A. Chang (1979). "Effect of surface roughness on the microwave emission from soils." Journal of Geophysical Research, Vol.81, pp.3660-3666.

Dalal, R. C., and R. J. Henry (1986). "Simultaneous determination of moisture, organic carbon, and total nitrogen by infrared reflectance spectrometry." *Soil Science Society of America Journal,* Vol.50, pp.120-123.

Georgakakos, K. P., D. H. Bae, and D. R. Cayan (1995). " Hydroclimatology of continental watersheds: 1. Temporal Analyses." *Water Resource Research,* Vol.31, No.3, pp.655-675.

Ghedira, H., T. Lakhankar, N. Jahan, and R. Khanbilvardi (2004). "Combination of passive and active microwave data for soil moisture estimates." *IEEE International Geoscience and Remote Sensing Journal,* Vol.4, pp.2783-2789.

Haby, J., (January, 2010). The soil moisture's impact on weather prediction. [online] April, 2011. http://www.theweatherprediction.com/habyhints/35/.

Haibin, L., A. Robock, and M. wild (2007). "Evaluation of intergovernmental panel on climate change fourth assessment soil moisture simulations for the second half of

the twentieth century." *Journal of Geophysical Research,* Vol.112, No.D06106, pp.1-15.

Huang, J., van den Dool, H. M., and K. P. Georgakakos (1996). "Analysis of model-calculated soil moisture over the United States (1931–1993) and applications to long-range temperature forecasts." *Journal of Climate,* Vol.9, No.6, pp.1350-1362.

Jackson, T. J. (1993). "Measuring surface soil moisture using passive microwave remote sensing." *Hydrological processes journal,* Vol.7, pp.139-152.

Jackson, T. J., T. J. Schmugge, A. D. Nicke, G. A. Coleman, and E. T. Engman (1981). "Soil moisture updating and microwave remote sensing for hydrological simulation." *Hydrological Science Bulletin,* Vol.26, No.3, pp.305-319.

James, E. A., (December 1999). Soil moisture. [online] April 2011. http://www.ghcc.msfc.nasa.gov/landprocess/lp_home.html. Nguyen, M., (2008). "Field estimation of soil water content: A practical guide to methods, instrumentation and sensor technology." Unpublished report of the International Atomic Energy Agency, VIENNA, Austia.

Owe, M., R. De Jeu, and J. P. Walker (2001). "A methodology for surface soil moisture and optical depth retrieval using the microwave polarization difference index." *IEEE Transactions on Geoscience and Remote Sensing Journal,* Vol.39, pp.1643-1654.

Sato, Y., and Katsushi I. (1994). "Reflectance analysis under solar illumination.". Research CMU-CS-94-221 by School of Computer Science/ Carnegie Mellon University. Pittsburg, Pennsylvania 15213-3890. http://www.dtic.mil/cgi bin/GetTRDoc?AD=ADA290489&Location=U2&doc=GetTRDoc.pdf

Said, S., U. C. Kothyari, and M. K. Arora (2008). "ANN-based soil moisture retrieval over bare and vegetated areas using ERS-2 SAR data." *Journal of Hydrologic engineering,* Vol.13, No.6, pp.461-475.

Schmugge, T. J., P. Gloersen, T. Wilheit, and F. Geiger (1974). "Remote sensing of soil moisture with microwave radiometers." *Journal of Geophysical Research,* Vol.79, No.2, pp.317-323.

Prichard, L.T. (n.d.). "Soil moisture measurement technology," University of California Davis, One Shields Avenue, Davis, CA 95616, USA. *ceeldorado.ucdavis.edu/files/45069.pdf*

Trenberth, K. E., G. W. Branstator, and P. A. Arkin (1988). "Origins of the 1988 North American drought." *Science Journal*, Vol.242, No.4886, pp.1640-1645.

Walker, J., (1999). *Estimating soil moisture profile dynamics from near- surface soil moisture measurements and standard meteorological data.* PH.D. Dissertation, University of Newcastle, Australia,.

Yeh, T. C., R. T. Wetherald, and S. Manabe (1984). "The effect of soil moisture on the short-term climate and hydrology change—A numerical experiment." *Monthly Weather Review*, Vol.112, pp.474-490.

CHAPTER 2

REVIEW AND EVALUATION OF REMOTE SENSING METHODS FOR SOIL MOISTURE ESTIMATION*

ABSTRACT

Soil moisture information plays an important role in disaster predictions, environmental monitoring, and hydrological applications. A large number of research papers have introduced a variety of methods to retrieve soil moisture information from different types of remote sensing data, such as optical or radar data.

The purpose of this study is to evaluate the most robust methods in retrieving soil moisture information from bare and vegetation-covered soil. This paper starts with an

introduction to the importance and challenges of soil moisture information extraction, and the development of soil moisture retrieval methods. An overview of soil moisture retrieval methods using different remote sensing data is presented either active, or passive, or a combination of both active and passive remote sensing data. The results of the methods are then compared. The advantages and limitations of each method are summarized.

The comparison shows that a statistical method gives the best results among others in the group a combination of both active and passive sensing methods: reaching a

---

* This paper is co-authored by Amer Ahmad, Yun Zhang and Sue Nichols and was published in the *SPIE Reviews Journal* on February 28, 2011. For the sake of clarity, the paper has been slightly edited.

1.83% gravimetric soil moisture (%GSM) RMSE and a 96% correlation between the estimated and the field soil measurements. In the group of active remote sensing methods, empirical models based on backscatter provide the best results giving a 2.32-1.81 % GSM RMSE and a 95%-97% correlation between the estimated and the field soil measurements. Finally, among the group of passive remote sensing methods, neural networks give the most desirable results: a 0.0937% GSM RMSE and a 100% correlation between the estimated and the field soil measurements. Overall, - neural networks applied to the passive remote sensing data achieves the best results among all the methods reviewed.

2.1 Introduction

2.1.1 Importance of Soil Moisture Information:

Estimating soil properties, including soil moisture, is important for many water budgeting processes, and for meteorological and agricultural applications [Verhoest et al., 2008]. Soil moisture information can also be used as an indicator for the prediction of natural disasters, such as flooding and droughts, and for environmental changes contributing to the information of dust storms and enhancing erosion [Canada Center for Remote Sensing, 2008]. However, accurately measuring soil moisture in-situ is expensive, because it requires a repeated sampling process. Moreover, the sampling itself may introduce problems making the sampled data unreliable [Lakhankar et al., 2006].

Remote sensing has the ability to collect high-quality information from large areas, repeatedly over very short time intervals (e.g. daily). This has been particularly the case with recent developments in sensor functionality and enhancement in both temporal and spatial image resolution.

2.1.2 Challenges of Soil Moisture Estimation

The task of estimating soil moisture becomes more difficult when the study area is covered with dense vegetation or snow, and when there are significant variation in topographical [Lakhankar et al., 2009; Sandells et al., 2008]. The most accurate results

are achieved when there is no or low vegetation cover, especially when the test area is flat. By considering vegetation cover and topography as the main parameters that affect soil moisture estimation, the question that needs to be answered is *why does soil covered with vegetation or snow, and with topographical changes, cause difficulty in estimating soil moisture accurately?*

The emitted electromagnetic radiation (in the passive remote sensing case) or the reflected microwave radiation (in the active remote sensing case) from the soil surface to the sensor represents the only measurement for studying the soil properties remotely. This emitted or reflected radiation from a covered soil surface to the remote sensor will no longer represent the actual soil surface emission because part of the emitted/reflected radiation might be either absorbed or enhanced by the vegetation cover [Du et al., 2000]. For topography, the surface roughness may be underestimated or overestimated as the surface will be either tilted toward or against the remote sensor [Dubois, 1995]. Therefore, spots in different locations may have different local incidence angles with respect to the sensor and might give unrealistic predictions.

From the remote sensing image interpretation point, when the value of a pixel has been acquired from a homogenous land cover, the value reflects the actual land cover where the pixel was captured. However, when a land area consists of a mixture of vegetation and bare soil cover, the pixels value reflects the mixture of land cover. Heterogeneity is defined as consisting of elements that are not of the same kind or nature [Miller, 2009]. Pixels values from different land cover cause confusion in assigning the exact pixel label to the right land cover, especially at large scales. Additionally, different

land cover reduces the classification accuracy of soil moisture retrieval and mixed-pixels values have better accuracy and a lower root mean square error (RMSE) in soil moisture classification [Lakhankar et al., 2006**;** Lakhankar et al., 2009].

In terms of the soil moisture estimation depth, remote sensing methods have been relatively successful in measuring the moisture at a depth of 5 cm in the soil for bare or nearly bare soil [Jackson, 1996; Dunne, 2007; Chauhan, 2003]. Meanwhile, estimating soil moisture at root zone depth, 10 cm or more from the surface, can be considered as another challenge.

For brevity, a number of acronyms have been used as follows: Moderate Resolution Imaging Spectroradiometer (MODIS), Synthetic Aperture Radar (SAR), Advanced Microwave Scanning Radiometer–EOS (AMSR-E), Earth Resources Satellite (ERS), Pushbroom Microwave Radiometer (PBMR), Japanese Earth Resources Satellite (JERS), Spaceborne Imaging Radar-C/X-band Synthetic Aperture Radar (SIR-C/X-SAR), Land Surface Temperature (T_s), Advanced Land Observing Satellite–PRISM and AVNIR instruments additional to L-band SAR (ALOS-PALSAR), Microwave Imaging Radiometer using Aperture Synthesis (MIRAS), Tropical Rainfall Measuring Mission/Microwave Imager (TRMM/TMI) remote sensing data, Electrically Scanning Microwave Radiometer (ESMR), Electro Magnetics Institute Radiometers (EMIRAD), and Advanced Space born Thermal Emission and reflection Radiometer (ASTER).

2.1.3 Sensors Development for Soil Moisture Estimation

Table 2.1 briefly describes the development of some of the satellites that have been widely used for soil moisture estimation since 1991.

Table 2.1 Satellites' Sensor Developments for Soil Moisture Estimation

Satellite	Sensor	Year launched	Owned by	Data type
Land sat	Land sat	1975	NASA	Passive
ESRI-1	SAR-C-band	July.1991	European space agency	Active
JERS-1	SAR-L-band	February.1992	Japanese Agency	Active
SIR-C/X-SAR	SAR	April.1994	U.S - German-Italian	Active
ERS-2	SAR	April.199	European space agency	Active
RADARSAT-1	SAR-C-band	November.1995	Canadian Space Agency	Active

Terra	MODIS- Terra	December.1999	NASA, partnerships with the aerospace agencies of Canada and Japan.	Passive
	ASTER- Terra		NASA, partnerships with the aerospace agency of Japan.	
Aqua	AMSR-E- Aqua	May.2002	NASA and the National Space Development Agency (JAXA) of Japan	Passive
	MODIS- Aqua			
ALOS-PALSAR	SAR L-band, PRISM, and AVNIR-2 instrument	January.2006	National Space Development Agency of Japan	Passive + Active
RADARSAT-2	SAR-C-band	December. 2007	Canadian Space Agency	Active
SMOS	MIRAS (interferometric radiometer) L-band	November.2009	European space agency	Passive

2.1.4 Purpose and Workflow of the Study

Different soil moisture evaluation methods have been introduced by different authors for different applications. The purpose of this study is to review, compare, and summarize existing methods to identify their effectiveness and weaknesses. The objective is to evaluate the methods that are applicable to land cover with mixed vegetation and bare soil.

The paper starts with an overview of the importance, the challenges and the development of estimating soil moisture information from remote sensing data. Then, an introduction to the remote sensing methods that are applied to estimating soil moisture information from different satellite imagery is presented. This is followed by an overview of different methods that are classified into three main groups based on remote sensing data used: group of active remote sensing methods, group of passive remote sensing methods, and group of combined of active and passive remote sensing methods. Some methods are used commonly in all the three groups. Then, a comparison of each group methods is presented, and the most robust method of all groups is identified. Finally, the results are discussed and a conclusion is drawn. The information that is presented in this paper is presented in Figure 1.1. The paper's main sections are drawn as trapezoidal shapes in the diagram, and the methods that are used in each remote sensing group are presented separately in rectangular shapes.

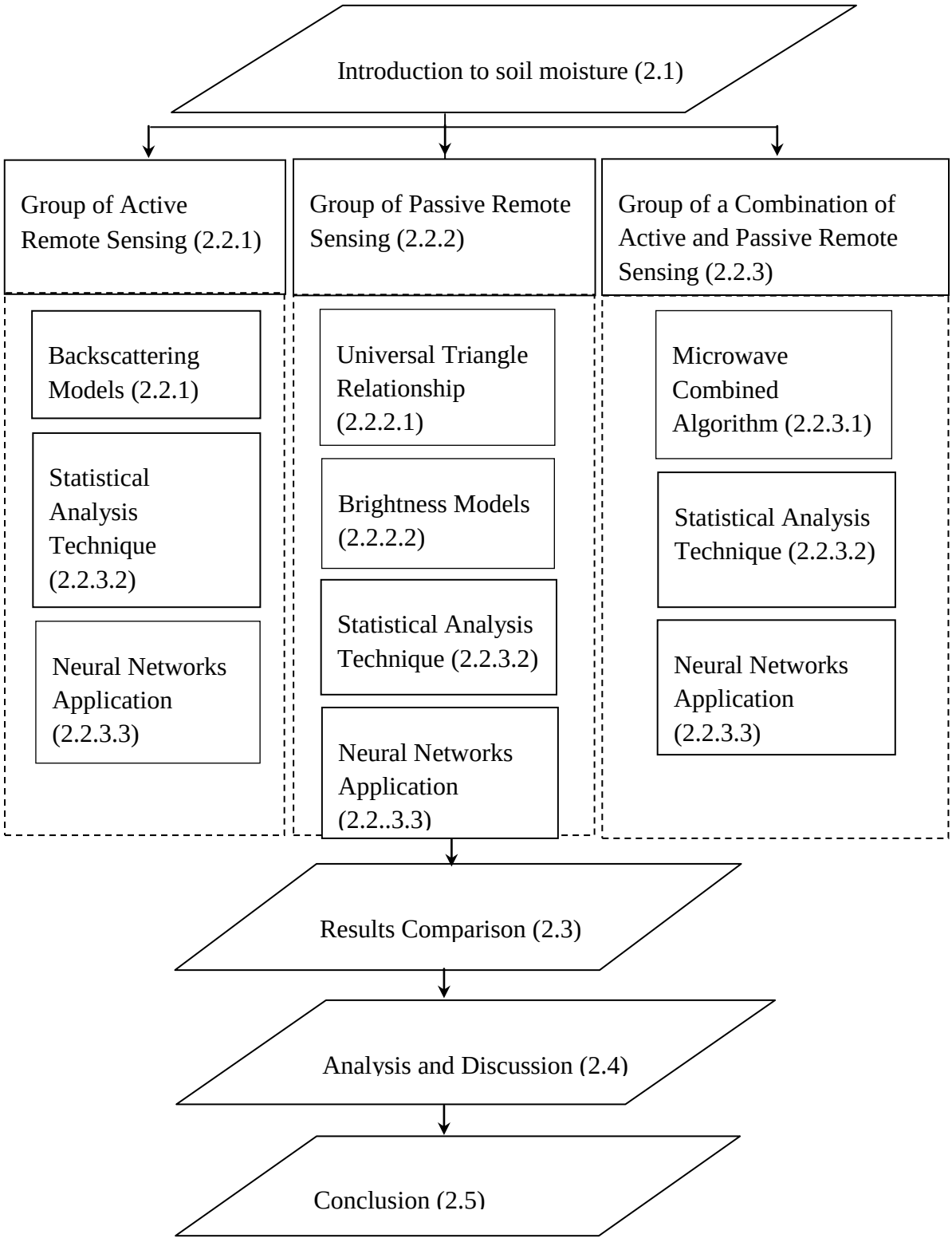

Figure 2.1 Presentation of the paper's content

2.2 Soil Moisture Retrieval Methods Using Remote Sensing

Soil moisture information can be retrieved from different remote sensing methods using different data such as visible, infrared, thermal, and microwave data [Batlivala and Ulaby, 1977]. Each remote sensing method used has its own advantages and disadvantages, based on how sensitive the soil surface is to the electromagnetic radiation and how strong the reflected radiation, from the soil surface, can be received by the sensor. Below is an overview, including pros, cons, and a comparison among three different remote sensing group of methods that have been widely applied in field of soil moisture estimation.

2.2.1 Group of Active Remote Sensing Methods

Electromagnetic microwave radiation with a wavelength that ranges between 0.5 cm and 100 cm has been used to measure the soil characteristics, using active remote sensing. Synthetic Aperture Radar (SAR) sensor, an active remote sensor, is the most widely used sensor for soil moisture estimation because of its ability to capture high resolution images for soil moisture based on the spatial variation in the ground soil moisture.

The operation's process is based on two main factors: sensor parameters and soil parameters. The sensor parameters factor is represented by the variations in signal backscatter as a function of wavelength, incidence angle, and polarization [Baghdadi et al., 2008; Smith et al., 2007]. The soil parameters factor is represented by the soil surface, the attenuation of the signal through the vegetation canopy, and the vegetation volume radiation backscatter [Ulaby et al., 1996]. Normally, the lower soil moisture content is in the soil surface, the stronger the radar backscatter value is under the same land cover conditions.

The backscatter signal (σ°) of an object is an amount of radiation reflected from the object's surface and measured by a unit area in radar cross section [Wagner, 1998]. In other words, it represents the amount of measured microwave radiation that was sent originally by a radar sensor towards an object and then reflected from the object's surface towards the radar sensor.

Like other active microwave sensors, SAR has the ability to penetrate the sub-layer under the soil surface [Prost, 2001]. SAR provides high spatial resolution images, normally tens of metres. Furthermore, the technique of capturing SAR imagery is not influenced by weather conditions. However, it has a low temporal frequency and is more sensitive to soil roughness and vegetation [Wang and Qu, 2009].

The following group of methods, which uses active remote sensing data, is widely used for soil moisture estimation:

- Backscattering models

- Statistical Analysis technique

- Neural Networks application

2.2.1.1 Backscattering Models

Backscattered signal σ° is received by the radar sensor as an electromagnetic microwave emission. Then backscatter radiation is converted to decibel values using the following formula [Baghdadi et al., 2007]:

$$\sigma^\circ_{dB} = 10 \log_{10} (\sigma^\circ) \quad (1.1)$$

For modeling the radar backscatter signal, three kinds of models have been used for soil moisture estimation: empirical models, semi-empirical models, and theoretical models.

Empirical Models: Empirical backscatter models result from several site experiment measurements of the backscatter signals (σ°) that are reflected from the soil surface to the radar sensor. The measured data are used to establish general boundaries or conditions that can be applied to obtain reasonably accurate soil moisture [Walker, 2004]. However, empirical models may not be applicable when the set of conditions is changed such as frequency, incidence angle, surface roughness, vegetation density, topography, etc. Therefore, they do not deliver desirable correlation results with the field measurement under a different set of conditions [Oh et al., 1992]. Some empirical models are designed

based on using different sensor polarization, which is either vertical or horizontal, to estimate soil roughness and soil moisture such as used in models proposed by Wang and Zhang [1995], Dubois et al.[1995], and Oh [1992].

Theoretical Models: Theoretical models are derived under restrictive theoretical basis to predict the general trend of radar backscatter in response to changes in soil roughness or soil moisture [Ulaby et al., 1996; Walker et al., 2004; Xiao and Zengxiang, 2005]. Theoretical backscatter models are good for describing the soil surface properties based on a theoretical perspective. In addition, these models can be applied at different soil characteristics using different sensor properties. However, it is difficult for theoretical models to represent all the architecture of the vegetation canopy in one model; therefore, some models are designed to present the leaf part only while others present the branch part only [Bindlish and Barros, 2001]. Theoretical modeling is sensitive to surface soil roughness and vegetation, and small deviations in soil roughness can cause large differences in the calculated backscatter; hence, these models are described as highly sensitive to signal backscatter [Thoma et al., 2006].

An example of widely used theoretical models is Kirchhoff models, which represent the relationship between geometrical optics and physical optics from radar backscatter [Dobson and Ulaby, 1986]. Chan et al. model is another widely used theoretical model [Chen et al., 2003].

Semi-Empirical Models: Semi-empirical models are derived from experimental data to develop empirical fitting of backscatter measurements for the soil surface [Bindlish and

Barros, 2001]. These models find an agreement between empirical models and theoretical models by having common rules derived from both models. Semi-empirical models provide a detailed description of radar backscatter of soil moisture, and they might be applied when little or no information about surface roughness for deriving these models is available [Ursoa and Minacapilli, 2006].

Oh et al. [2002] proposed a semi-empirical model of the ensemble-averaged differential Mueller matrix, which uses backscatter signal on bare soil. The two other commonly used soil moisture retrieval methods, statistical analysis technique and neural networks, are explained in sections 2.3.2 and 2.3.3, respectively.

2.2.2 Group of Passive Remote Sensing Methods

Modeling soil moisture using passive remote sensing information has made a large impact on mapping the global soil moisture, as it is the best method for representing the global soil moisture distribution [Jackson and Schmugge, 1991].

This group of methods retrieves soil moisture information independently even when there is a vegetation canopy available [Wang et al., 2007]. It provides information about the land properties such as surface temperature and Normalized Difference Vegetation Index (NDVI). In addition, passive microwave systems have the ability to cover a large surface area with a low spatial resolution, normally tens of kilometres.

However, some researchers imply that the Optical/IR method has the advantage of providing fine spatial resolution for soil moisture estimation [Carlson, 2007]. The thermal infrared band, which ranges from 3 to 14 μm, is the electromagnetic wavelength that measures the land characteristics in this group of methods. These methods have proven their ability to retrieve soil moisture information independently by providing direct measurements for soil moisture [Walker et al., 1997]. The first attempt to estimate soil moisture from passive remote sensing information was proposed by Jackson [Walker and Houser, 2001], whose method was adopted to calculate soil moisture retrieval for the top metre of the soil. Later, many applications have been proposed based on establishing a relationship among land parameters, vegetation indices, and surface radiant temperature measurements [Choudhury et al., 1995; Owen et al., 1998].

The following group of methods, which uses passive remote sensing data, is widely used for soil moisture estimation:

- Universal triangle relationship method
- Brightness models
- Statistical Analysis technique
- Neural Networks application

2.2.2.1 Universal Triangle Relationship Method

The universal triangle relationship is a widely used method for modeling different soil- vegetation cover areas. It was proposed by Carlson et al. [1994] and Gillies et al. [1997] after they had conducted many trial experiments.

The method shows that there is a universal relationship among soil moisture, NDVI, and land surface temperature (T_s) of a given region. The shape of the relationship is triangular or a slightly truncated trapezoidal, Figure 2.2. The upper left edge, red color zone, is represented by pixels having low moisture content with low vegetation and high temperature “dry edge”; most of these pixels are representative of bare soil. The middle zone area, orange color, represents pixels having partially vegetative cover and low moisture content with an average temperature. The lower right edge, green color zone, represents pixels representative of densely vegetated covered with high soil moisture and low temperature called “wet edge”. Hence, every pixel in an image will be presented within the range between warm and wet edge of the drawn triangle, and located in the triangle depending on how moist and vegetated the area is.

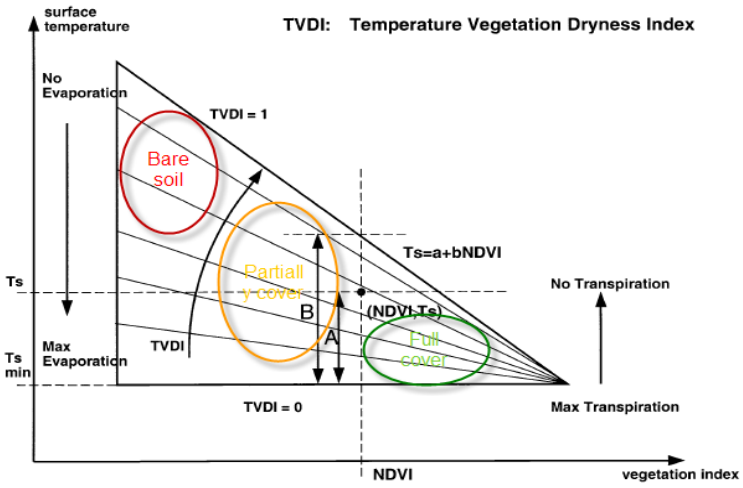

Figure 2.2 T_s-NDVI representation for the Universal Triangle Method (after Sandholt et al. [2002, p. 216]).

The relationship among the three parameters is presented in the following regression formula [Carlson, 2007].

$$M = \sum_{i=0}^{i=n} \sum_{J=0}^{j=n} a_{ij} NDVI^{*(i)} T^{*(j)} \tag{1.2}$$

where a_{ij} is the regression coefficient.

Although the method is based on optical remote sensing data, which is influenced by atmospheric conditions, the universal method is insensitive to surface conditions, atmosphere, and net radiation [Walker et al., 1997]. Furthermore, the method requires a simple process to extract the ground soil moisture information [Carlson, 2007].

Other indexes have been derived based on the method's principles such as TVWI [Hassan et al., 2007]. Many other studies have followed this method such as Sandholt's method [2002] and Wang et al. method [2007]. The method's limitation is that it is affected by topographic changes; therefore, the land surface where the triangular shape will be identified must be flat [Walker et al., 1997].

2.2.2.2 Brightness Models

Brightness models, also called radiometric models, give better estimation results on bare soil as the surface emission radiation reflects the soil's dielectric properties. Brightness temperature (T_B) represents the model's main input parameter; T_B is the amount of measured radiation, in terms of temperature, from an object's surface to the sensor. Additional data such as the vegetation parameters and the surface parameters, like bulk density and soil texture, can be added to improve the model's output results. Another important soil parameter that affects these models is the soil roughness, which is represented by root-mean-square (RMS) height and the correlation length [Verhoest et al., 2008; Nishimoto, 2008].

Compared to the modeling applications, radiometric models are relatively easy to implement and do not need field experiments [Jackson, 1993]. However, their use is more limited to a specific case or available data. Many brightness models were proposed for

retrieving soil moisture from passive data [Bindlish et al., 2003; Jackson et al., 1999; Blanchard et al., 1981]. Shi et al. [2006] model is another example based on the relationship between surface microwave brightness temperature and the physical surface temperature. The other two commonly used methods, which are statistical analysis technique and neural networks application, will be addressed later (in section 2.3.2 and in section 2.3.3).

2.2.3 Group of Combined Active and Passive Remote Sensing Methods

As remote sensing instruments and spacecrafts have been developed, integrating both active and passive remote sensing information with their particular strengths and weaknesses has become worthwhile. Thus combining high spatial resolution information from active remote sensing with high temporal resolution information from passive remote sensing on an extended area has improved the soil moisture estimation accuracy. In addition, the revolution of developing advanced spacecrafts, which are designed to carry many sensors, both passive and active, enabled integrating both data in one system, such as ALOS-PALSAR and Soil Moisture Active and Passive (SMAP) mission (planned to be launched in 2014). The first algorithm that used the advantages of this method was implemented by O'Neil [O'Neill et al., 1996]. It has been found that the results improved substantially as compared to individually used data. As a result, many researches follow the technique of integrating both active and passive methods for soil moisture estimation.

The most widely used group of methods, which combines both active and passive data, is listed below:

- Microwave combined algorithms

- Statistical Analysis technique

- Neural Networks application

2.2.3.1 Microwave Combined Algorithms

Normally, soil moisture estimation algorithms analyze the pixels' digital number (DN) after making sure that the effects of atmosphere, vegetation, geometry, soil properties, and sensor configurations have been corrected. Later, the algorithm that establishes an objective relationship between the estimated and the field soil moisture measurements may be initiated.

Integrating information from both passive and active remote sensing data in a complementary way to reach a new level of accurately estimated results is the main aim of this methodology. A combined algorithm includes input parameters extracted from active remote sensing such as vegetation and surface roughness, and parameters extracted from passive remote sensing such as brightness temperature (T_B.). In most cases, the

algorithm also considers essential soil moisture parameters that affect the estimated soil moisture accuracy, such as optical depth and surface roughness [Chauhan, 1997].

A workshop report released by NASA Soil Moisture community for Active/Passive (SMAP) Mission implies that combined algorithms are not as robust as the brightness passive algorithms [NASA, 2009]. However, combining active with passive method, such as SAR and radiometer, can reduce soil moisture prediction errors by ±30% of the true field capacity [Ulbay et al., 1983].

2.2.3.2 Statistical Analysis Technique

All kinds of remote sensing data that have been mentioned above can be used in the methods for soil moisture estimation. This method uses statistical calculations on the data to draw a relationship between two variables: the estimated soil moisture from the remote sensing information and the field soil moisture. Most of this statistical analysis is represented by a linear regression analysis, which is widely used between the two variables [Bolten et al., 2003]. Many statistical methods that have been implemented to retrieve soil moisture are based on converting the emitted microwave radiation, from the surface to the sensor, into mathematical values that can be statistically analyzed [Bolten et al., 2003; Sanden et al., 1996]. The regression analysis aims to measure the degree of linear correlation between the two variables. The more linear the relationship is, the

better the correlation between the estimated soil moisture and the measured soil moisture. Kauzar et al. [2006] proposed a regression analysis method based on the regression method to form a relationship between the L-Band emission of the biosphere model (L-MEB) and the retrieved soil moisture using a semi-empirical regression method [Saleh et al., 2006]. Another statistical retrieval method was presented by Pellarin et al. (2003); it was aimed at finding the relationship between T_B and the retrieved soil moisture [Pellarin et al., 2003].

2.2.3.3 Neural Networks Application

Neural networks are an artificial intelligence technique that consists of a set of mathematical functions that complement each other to produce a desirable output result.

Several studies describe neural networks application as an inverse model because it converts the input information into desirable output results [Wignerona et al., 2003; Chuah and Chong, 1993; Ushada et al., 2007]. In general, neural networks are based on series of complex mathematical equations applied to the network's input parameters to deliver desirable output results. Neural networks applications are widely used in different fields of science such as medical applications, weather forecasting, and other computer applications.

In the field of remote sensing, one of the most important kinds of neural networks is the back propagations network due to the application's ability to produce more desirable results. Moreover, for soil moisture estimation, both active and passive remote sensing information have shown desirable results using this method.

The methodology's drawback is that under a vegetated area the neural networks application gives inaccurate results due to a lack of correlation between the backscattered radiation and the in situ soil measurements [Lakhankar et al., 2009]. Furthermore, the neural networks application has a complex computation network to design a desirable correlation between the input and the output results because the application is highly sensitive to the input parameters [Ghedira et al., 2004]. As a result, it requires the user's experience to integrate adequate input parameters and carefully choose the acquired training pixels without overtraining to get better output accuracy.

Table 2.2 Results of Group of Combined Active and Passive Remote Sensing Methods

Reference	Methodology	RMSE (%GSM)	CR %
[Chauhan, 1997]	A microwave combined algorithm	-	Min. of 93
[Bindlish and Barros, 2002]	- A retrieval algorithm - An inverse model	- 3.16 for ESTAR - 3.78 for SAR	-
[Notarnicola et al., 2006]	A Bayesian inversion model	-	

			- 68 For C-band - 60 For L-band
[Lakhankar et al., 2009]	- Fuzzy logic + - Neural networks	- 3.39 - 5.5	-
[Ghedira et al., 2004]	Neural networks	-	77
[Lakhankar et al., 2009]	- Neural networks + - Fuzzy logic	- 6.44 - 6.97	-
[Bolten et al., 2003]	A statistical regression analysis	1.83	96
	A statistical regression analysis	2.63	67
	Passive physical model	2.23	90
	Active physical model	2.79	64

Wigneron et al. [2003] describe neural networks application as a simple and efficient method in passive remote sensing observations for soil moisture estimation, and they imply that the application can only be limited for the regions and the time period during which they were calibrated [Wignerona et al., 2003].

2.3 Results Comparison

In order to evaluate the accuracy of each soil moisture estimation method, a general statistical analysis based on the correlation coefficient (CR) and/or the standard deviation (RMSE) was conducted in Tables 3, 4, and 5. The analysis was compared between the estimated result and the corresponding field measurement. A linear correlation between the estimated result and the field data was drawn in a two-dimensional scatterplot, and then the correlation coefficient was calculated. When the correlation coefficient is high and the standard deviation is low, the method is considered robust and the analysis result is more desirable, and vice versa.

The comparison process is implemented based on classifying the group of methods based on the remote sensing data used: The active remote sensing group, the passive remote sensing group, and a combination of active and passive remote sensing group. Based on the statistical analysis that is shown in tables 2.3, 2.4 and 2.5, the most robust method in each group was chosen, and then the best method among the chosen methods was identified as the most successful method.

The CR of each method was calculated based on the number of soil samples measured and the correspondent number of correspondent points in the analysis results.

The land cover conditions and the surface parameters considered for each study area are identified for each reference.

Table 2.3 Results of Group of Active Remote Sensing Methods

Reference	Methodology	RMSE (%GSM)	CR %
[Haider et al., 2004]	An empirical model	-	- 89For bare soil 75For vegetated soil - 83For combined data
[Said et al., 2006]	An empirical model + A nonlinear least square method	2.32- 1.81	95 -97
[Sprintsin et al., 2002]	A backscatter theoretical model	-	- 96For Sandy soil - 97For loess soil
[Dubois et al., 1995]	An empirical algorithm	< 4.2	-
[Said et al., 2008]	Neural Networks	4	90

Table 2.4 Results of Group of Passive Remote Sensing Methods

Reference	Methodology	RMSE (%GSM)	CR %
[Carlson, 2007]	Universal Triangle Relationship	<0.07	40 -96
[Wen et al., 2003]	An analytic algorithm	-	80

[Liou et al., 2001]	Neural Networks + a land surface process/radio brightness model	0.0937	1
[Blanchard et al., 1981]	An algorithm	-	71.6
[Vecchia et al., 2007]	A transfer Model (Emission model)	2.56	84

The appendix table contains more detailed information about the soil cover types of the study area as well as the soil parameters that are considered in each paper presented above. For instance, some researchers considered vegetation parameters or topography changes to determine their effect on the estimated results, while others did not.

2.4 Analysis and Discussion

Results from a number of soil moisture estimation methodologies are compared according to the data used under a similar land cover, which is bare and vegetation-covered soil. In all cases, each author found his/her proposed method works well compared with other selected methods. The comparison guides among different methods in each group are based on statistical parameters, such as a correlation coefficient and/or an RMSE between the methods' estimated results and the field measurements. Based on the difference in soil parameters considered in each methodology, such as the area's

topography and the vegetation density, it is difficult to draw an absolute conclusion about which one is the best and which one is the worst. However, each method to estimate soil moisture is fairly applicable in different areas as it is applicable under different land conditions. Land cover conditions have a substantial effect on the final soil moisture information estimation because of the significant effect of vegetation on the sensor's backscatter radiation.

In addition, different methods use different ways of collecting the in situ soil measurements, and the number of collected soil measurements in each method is different from others. Therefore, in each reference presented, the statistical parameters were calculated based on the number of collected measurements. Moreover, the numbers of collected measurement might affect the calculated statistical parameters. For instance, a few numbers of collected measurements might give a higher correlation with the estimated points, whereas the number of measurements increases, the correlation coefficient might decrease.

Based on the presented statistical parameters, the methods can be ranked from the lowest RMSE and higher CR, which is the most robust method to the higher RMSE and lower CR, which is the less robust method. However, other parameters such as the difference in method of collecting the measurement and the difference in the number of measurements that are used to calculate the statistical parameter could cause misleading results in ranking the methods accurately.

Based on the statistical parameters values that are presented in table 2.3 2.4 and 2.5, some general observations can be made for each group of methods used. First, among the active remote sensing group, the radar backscatter modeling method gives desirable estimation results.

Second, neural networks modeling gives a better result compared with other group of passive remote sensing methods, and its result is the best among all methods.

Third, a statistical analysis method on data captured from soil moisture satellites such as PALS has delivered highly correlated results for soil moisture estimation using data captured by radiometric passive channels rather than scaterometer channels. Additionally, ground soil measurements at a few centimetres' depth (0-1 cm) from the field surface layer gives better correlation with the estimated soil moisture compared with the ground measurements at deeper layers.

Fourth, in bare soil, using active remote sensing gives a more accurate correlation result with the field soil measurements than all other methods, without necessarily considering the soil roughness effect.

Finally, the surface scattering method in bare soil is usually related to geometric and dielectric properties, which affects the backscattered radiation response substantially. Moreover, correcting the vegetation optical parameters plays a significant role in increasing the moisture estimation accuracy of a vegetation-covered soil.

From the observations above, a few general recommendations can be made. If both sensor parameters and land cover properties are important for having highly accurate

results, a relationship between these two main variables needs to be drawn. Moreover, based on the results compared above, for a vegetation-covered soil, the most accurate result is found when neural networks application is used. Although all the mentioned methodologies have the capability to retrieve soil moisture at certain conditions and have their strengths and weaknesses, estimating soil moisture using remote sensing cannot be replaced by the actual soil field measurements.

2.5 Conclusion

In this study, an assessment of the current methodologies for soil moisture estimation was performed based on their common soil cover conditions. Other soil surface parameters, which are not considered in this comparison, might affect the comparison results, such as the topographical area, the method of collecting the field measurements, and the number of collected in situ measurements. Some of those parameters have not been considered in this study because either they were unknown or they were neglected and no correction was made to consider their effect. Therefore, vegetation parameters have more attention than topography parameters.

At present, remote sensing methods have not been successful in estimating soil moisture from deep soil layers, such as at the root zone soil layers. However, the ability to retrieve soil moisture information from the surface layers in itself needs to be further investigated.

Even though in situ soil moisture measurements might involve a sampling error, they are considered the standard measurements of soil moisture, and as a result remote sensing based estimates are usually compared with the field measurements.

Based on the active remote sensing methods, estimating soil moisture on bare soil or soil with less vegetation gives more accurate results, as compared to using the methods on a mixture of land cover. Moreover, the estimation process becomes more challenging when the vegetation cover is dense. In contrast, under similar soil cover conditions, retrieving soil moisture using a combination of both active and passive soil information gives reasonably accurate results. Processing the captured microwave signal to convert it to mathematical values, then implementing a mathematical algorithm or a model to correct the soil surface and sensor parameters, then analyzing the output results using a statistical method are the main processing steps for the most widely used methodologies.

Acknowledgments

The author would like to thank the Iraqi Ministry of Higher Education for its sponsorship, and Krista Amolins, a PhD student at the Geodesy and Geomatics Engineering/ University of New Brunswick, for her support and feedback to make this paper better.

References

Baghdadi, N., M. Zribi, C. Loumagne, P. Ansart, and T. P. Anguela (2008). "Analysis of Terra SAR-X data and their sensitivity to soil surface parameters over bare agricultural fields." *Remote Sensing of Environment,* Vol.112, pp.4370-4379.

Baghdadi, N., M. Aubert, O. Cerdan, L. Franchistéguy, C. Viel, E. Martin, and Zribi, Mehrez Desprats, Jean François (2007). "Operational mapping of soil moisture using Synthetic Aperture Radar data: Application to the touch basin (France)." *Sensors Journal.*, Vol.7, pp.2458-2483.

Batlivala, P. P., and Ulaby F. T. (1977). "Feasibility of monitoring soil moisture using active microwave remote sensing." Unpublished report of the University of Kansa center for research, INC., remote sensing laboratory technical report,.

Bindlish, R., and A. P. Barros (2002). "Sub-pixel variability of remotely sensed soil moisture: An inter-comparison study of SAR and ESTAR." *IEEE Xplore Journal,* Vol.40, No.2, pp.326-337.

Bindlish, R., T. J. Jackson, E. Wood, H. Gao, P. Starks, D. Bosch, and V. Lakshmi (2003). "Soil moisture estimates from TRMM microwave imager observations over the southern United States." *Remote Sensing of Environment,* Vol.85, pp.507-515.

Bindlish, R., and A. P. Barros (2001). "Parameterization of vegetation backscatter in radar-based, soil moisture estimation." *Remote Sensing of Environment,* Vol.76, pp.130-137.

Blanchard, B. J., M. J. McFmland, T. J. Schmugge, and E. Rhoades (1981). "Estimation of soil moisture with API algorithms and microwave emission." *Water Resources Bulletin of American Water Resources Association,* Vol.17, No.5, pp.767-774.

Bolten, J. D., V. Lakshmi, and E. G. Njoku (2003). "Soil moisture retrieval using the passive / active Land S-Band radar/ radiometer." *IEEE Transaction and Geoscience in Remote Sensing,* Vol.41, No.12, pp.2792-2801.

Canada center for remote sensing, (February 2008). Fundamentals of remote sensing applications. [online] April 2011. http://www.ccrs.nrcan.gc.ca/resource/tutor/fundam/chapter5/14_e.php.

Carlson, T. (2007). "An overview of the "Triangle Method" for estimating surface evapotranspiration and soil moisture from satellite imagery." *Sensors Journal,* Vol.7, pp.1612-1629.

Chauhan, N. S., S. Miller, and P. Ardanuy (2003). "Spaceborne soil moisture estimation at high resolution: a microwave optical/IR synergistic method." *International Journal of Remote Sensing,* Vol.24, No.22, pp.4599-4622.

Chauhan, N. S. (1997). "Soil moisture estimation under a vegetation cover: combined active passive microwave remote sensing method." *international journal of remote sensing,* Vol.18, No.5, pp.1079-1097.

Chen, K. S., T. Wu, L. Tsang, Q. Li, J. Shi, and A. K. Fung (2003). "Emission of rough surfaces calculated by the integral equation method with comparison to three-dimensional moment method simulations." *IEEE Transactions on Geoscience and Remote Sensing Journal,* Vol.41, No.1, pp.90-101.

Choudhury, B. J., Y. H. Kerr, E. G. Njoku, and P. Pampaloni "1995). "Passive microwave remote sensing of land-atmosphere interactions." VSP, Utrecht, The Netherlands, Tokyo, Japan, .

Chuah, H. T., and T. O. Chong (1993). "Retrieval of soil moisture content from radar backscatter coefficients." *IEEE International Geoscience and Remote Sensing Journal,* Vol.1, pp.338-340.

Claudia, N., A. Mariella, and P. Francesco (2006). "Use of radar and optical remotely sensed data for soil moisture retrieval over vegetated areas." *IEEE Transactions on Geoscience and Remote Sensing Journal,* Vol.44, No.4, pp.925-935.

D'Ursoa, G., and M. Minacapilli (2006). "A semi-empirical approach for surface soil water content estimation from radar data without a-priori information on surface roughness." *Journal of hydrology,* Vol.321, pp.297-310.

Dobson, M. C., and F. T. Ulaby (1986). "Active Microwave soil moisture research." *IEEE Transactions on Geoscience and Remote Sensing Journal,* Vol.GE-24, No.1, pp.23-36.

Du, Y., F. T. Ulaby, and M. C. Dobson (2000). "Sensitivity to soil moisture by active and passive microwave sensors." *IEEE Transaction on Geoscience and Remote Sensing,* Vol.38, No.1, pp.105-113.

Dubois, P. C., and Z. J. Van "1994). "An empirical soil moisture estimation algorithm using imaging radar." In Proceedings, International Geoscience and Remote Sensing Symposium (IGARSS), .

Dubois, P. C., J. Zyl, and T. Engman (1995). "Measuring soil moisture with imaging radars." *IEEE Transaction on Geoscience and Remote Sensing Journal,* Vol.33, No.4, pp.915-926.

Dunne, S. C., D. Entekhabi, and E. G. Njoku (2007). "Impact of multiresolution active and passive microwave measurements on soil moisture estimation using the ensemble Kalman smoother." *IEEE transactions on Geoscience and remote sensing,* Vol.45, No.4, pp.1016-1028.

Fawwaz, T., M. Ulbay, C. Dobson, and D. R. Brunfeldt (1983). "Improvement of moisture estimation accuracy of vegetation-covered soil by combined active/passive microwave remote sensing." *IEEE Transactions on Geoscience and Remote Sensing Journal,* Vol.GE-21, No.3, pp.300-307.

Ghedira, H., T. Lakhankar, N. Jahan, and R. Khanbilvardi (2004). "Combination of passive and active microwave data for soil moisture estimates." *IEEE International Geoscience and Remote Sensing Journal,* Vol.4, pp.2783-2786.

Haider, S. S., S. Said, U. C. Kothyari, and M. K. Arora (2004). "Soil moisture estimation using ERS-2 SAR data: A case study in the Solani River catchment." *Hydrological sciences journal,* Vol.49, No.2, pp.323-334.

Hassan, Q. K., C. P. Bourque, F. Meng, and R. M. Cox (2007). "A wetness index using terraincorrected surface temperature and normalized difference vegetation index derived from standard MODIS products: An evaluation of its use in a humid forest-dominated region of eastern Canada." *Sensors Journal,* Vol.7, No.10, pp.2028-2048.

Jackson, T. J., and T. J. Schmugge (1991). "Vegetation effects on the of soils microwave emission." *Remote sensing of environment,* Vol.36, pp.1413-1418.

Jackson, T. J. (1980). "Profile soil moisture from surface measurements." *Journal of Irrigation Drainage Engineering,* Vol.IR-2, No.ASCE, pp.81-92.

Jackson, T. J., J. Schmugge, and E. T. Engman (1996). "Remote sensing applications to hydrology: Soil moisture." *Journal of Hydrological Sciences,* Vol.41, No.4, pp.517-529.

Jackson, T. J., D. M. Le Vine, A. Y. Hsu, A. Oldak, P. J. Starks, C. T. Swif, J. D. Isham, and M. Haken (1999). "Soil moisture mapping at regional scales using microwave radiometry: The southern great plains hydrology experiment." *IEEE Transactions on Geoscience and Remote Sensing Journal,* Vol.37, No.5, pp.2136-2151.

Jackson, T. J. (1993). "Measuring surface soil moisture using passive microwave remote sensing." *Hydrological Processes Journal,* Vol.7, No.2, pp.139-152.

Lakhankar, T., H. Ghedira, M. Temimi, A. E. Azar, and R. Khanbilvardi (2009). "Effect of land cover heterogeneity on soil moisture retrieval using active microwave remote sensing data." *Journal of Remote Sensing,* Vol.1, pp.80-91.

Lakhankar, T., H. Ghedira, M. Temimi, M. Sengupta, R. Khanbilvardi, and R. Blake (2009). "Non-parametric methods for soil moisture retrieval from satellite remote sensing data." *Journal of Remote Sensing,* Vol.1, pp.3-21.

Liou, Y., S. Liu, and W. Wang (2001). "Retrieving soil moisture from simulated brightness temperatures by a neural network." *IEEE Transaction and Geoscience in Remote Sensing,* Vol.39, No.8, pp.1662-1672.

Miller, G. A., (December 2009). WordNet open source. [online] January 2010. http://www.google.ca/search?hl=en&defl=en&q=define:heterogeneity&ei=7LW8SqeCIJDElAfIoOWYBA&sa=X&oi=glossary_definition&ct=title.

NASA workshop report, (2007). "Soil moisture active/passive (SMAP) mission." Unpublished report of the NASA, Arlington, Virginia, USA.

Nishimoto, M. (2008). "Error analysis of soil roughness parameters estimated from measured surface profile data." *IEEE Xplore journal,* Vol.II, pp.719-722.

Oh, Y., K. Sarabandi, and F. T. Ulaby (1992). "An empirical model and an inversion technique for radar scattering from bare soil surfaces." *IEEE Transactions on Geoscience and Remote Sensing Journal,* Vol.30, No.2, pp.370-381.

Oh, Y., K. Sarabandi, and F. T. Ulaby (2002). "Semi-empirical model of the ensemble-averaged differential Mueller matrix for microwave backscattering from bare soil surfaces." *IEEE Transactions on Geoscience and Remote Sensing Journal,* Vol.40, No.6, pp.1348-1355.

O'Neil, P. E. (1996). "Use of active and passive microwave remote sensing for soil moisture estimation through corn." *International journal of remote sensing,* Vol.17, No.10, pp.1851-1865.

Owen, T. W., T. N. Carlson, and R. R. Gillies (1998). "An assessing soil moisture of satellite remotely-sensed land cover parameters in quantitatively describing the climatic effect of urbanization." *International journal of remote sensing,* Vol.19, No.9, pp.1663-1681.

Pellarin, T., J. Wigneron, J. -. Calvet, and P. Waldteufel "2003). "Global soil moisture retrieval from a synthetic L-band brightness temperature data set." Journal of Geophysical Research (in press), .

Prost, G. L., (2001). "Remote sensing for geologists: A guide to image interpretation." Chapter , Gordon and Breach Science Publishers, Second edition, New York, .

Said, S., U. C. Kothyari, and M. K. Arora (2006). "Soil moisture estimation from ERS-2 SAR data in Solani River catchment." *Agriculture and Hydrology Applications of Remote Sensing Journal,* Vol.6411, pp.1-11.

Said, S., U. C. Kothyari, and M. K. Arora (2008). "ANN-based soil moisture retrieval over bare and vegetated areas using ERS-2 SAR data." *Journal of Hydrologic engineering,* Vol.13, No.6, pp.461-475.

Saleh, K., J. Wigneron, P. de Rosnay, J. Calvet, and Y. Kerr (2006). "Semi-empirical regressions at L-band applied to surface soil moisture retrievals over grass." *Remote Sensing of Environment,* Vol.101, pp.415-426.

Sandells, M. J., I. J. Davenport, and R. J. Gurney (2008). "Passive L-band microwave soil moisture retrieval error arising from topography in otherwise uniform scenes." *Advances in Water Resources,* Vol.31, pp.1433-1443.

Sanden, E. M., C. M. Britton, and J. H. Everitt (1996). "Total ground-cover estimates from corrected scene brightness measurements." *Photogrammetric engineering & remote sensing,* Vol.62, No.2, pp.147-150.

Sandholt, I., K. Rasmussen, and J. Andersen (2002). "A simple interpretation of the surface temperature/ vegetation index space for assessment of surface moisture status." *Remote Sensing of Environment,* Vol.79, pp.213-224.

Shi, J., L. Jiang, L. Zhang, K. S. Chen, J. Wigneron, A. Chanzy, and T. J. Jackson (2006). "Physically based estimation of bare-surface soil moisture with the passive radiometers." *IEEE Transactions on Geoscience and Remote Sensing Journal,* Vol.44, No.11, pp.3145-3153.

Smith, A. M., K. Scipal, and W. Wagner (2007). *Active sensor system for drought stress monitoring.* Agriculture and agri-food Canada Lethbridge, Alberta, Canada and institute of photogrammetry and remote sensing at University of Technology Vienna, Austria, [online].January 2010. ftp://193.43.36.44/agl/agll/ladadocs/activesensor.doc.

Sprintsin, M., D. G. Blumberg, J. B. Asher, J. Daniels, and M. Linetsky (2002). "Estimation of soil water content in the Negev desert open areas using archived ERS SAR images." *IEEE Xplore journal,* Vol.4, pp.2220-2222.

Tarendra, L., H. Ghedira, A. Azar, and R. Khanbilvardi (2006). "Effect of sub-pixel variability and land-cover on soil moisture retrieval from RADARSAT-1 data." *IEEE Xplore Journal,* pp.187-192.

Thoma, D. P., M. S. Moran, R. Bryant, M. Rahman, C. D. Holifield-Collins, and S. Skirvin (2006). "Comparison of four models to determine surface soil moisture from C-band radar imagery in a sparsely vegetated semiarid landscape." *Water Resources Research,* Vol.42, No.W01418, pp.1-12.

Ulaby, F. T., P. C. Dubois, and Z. J. Van (1996). "Radar mapping of surface soil moisture." *Journal of Hydrology,* Vol.184, pp.57-84.

Ushada, M., H. Murase, and H. Fukuda (2007). "Non-destructive sensing and its inverse model for canopy parameters using texture analysis and artificial neural network." *Computers and Electronics in Agriculture,* Vol.57, pp.149-165.

Vecchia, A. D., P. Ferrazzoli, J. -. Wigneron, and J. P. Grant (2007). "Modeling forest emissivity at L-band and a comparison with multitemporal measurements." *IEEE Geoscience and Remote Sensing Letters,* Vol.4, No.4, pp.508-512.

Verhoest, N. E. C., H. Lievens, W. Wagner, J. Álvarez-Mozos, M. S. Moran, and F. Mattia (2008). "On the soil roughness parameterization problem in soil moisture retrieval of bare surfaces from Synthetic Aperture Radar." *Sensor Journal,* Vol.8, pp.4213-4248.

Wagner, W., (1998). *Soil moisture retrieval from ERS scatterometer data.* Ph.D. Dissertation, Technisch-Naturwissenschaftliche Fakultät at the Vienna University of Technology, Karlsplatz 13, A-1040 Wien, Austria,.

Walker, J. P., P. R. Houser, and G. R. Willgoose (2004). "Active microwave remote sensing for soil moisture measurement: A field evaluation using ERS-2." *Hydrological Processes journal,* Vol.18, pp.1975-1997.

Walker, J. P., and P. R. Houser (2001). "A methodology for initializing soil moisture in a global climate model: Assimilation of near-surface soil moisture observations." *Journal of Geophysical Research,* Vol.106, No.D11, pp.11761-11774.

Wang, L., J. J. Qu, S. Zhang, X. Hao, and S. Dasgupta (2007). "Soil moisture estimation using MODIS and ground measurements in eastern China." *International Journal of Remote Sensing,* Vol.28, No.6, pp.1413-1418.

Wang, L., and J. J. Qu (2009). "Satellite remote sensing applications for surface soil moisture monitoring: A review." *Frontiers of earth Science in China,* Vol.3, No.2, pp.237-247.

Wen, J., Z. Sue, and Y. Ma (2003). "Determination of land surface temperature and soil moisture from tropical rainfall measuring mission/microwave imager remote sensing data." *Journal of geophysical research,* Vol.108, No.D2, pp.ACL 2-1-ACL 2-10.

Wignerona, J. -., J. -. Calvetb, T. Pellarinb, A. A. Griendc, M. Bergerd, and P. Ferrazzolie (2003). "Retrieving near-surface soil moisture from microwave radiometric observations: Current status and future plans." *Remote Sensing of Environment,* Vol.85, pp.489-506.

Xiao, W., and Z. Zengxiang (2005). "A review: theories, methods and development of soil moisture monitoring by remote sensing." *Proceedings of IGARSS journal,* Vol.6, pp.4505-4507.

Appendix I

Soil Characteristics of Each Reference Presented

Reference	Data source type	Soil cover type	Parameters considered	Comment
[Chauhan, 1997]	AirSAR + PBMR	Forest, permanent pasture, hay, corn, soybeans, senescent small grain crops and large flat corn fields	Optical depth and vegetation parameters,	Vegetation and surface roughness characteristics are assumed to remain constant
[Bindlish and Barros, 2002]	ESTAR + SAR	Rangeland, pasture, winter wheat, corn and alfalfa	Texture, vegetation parameters, topography, roughness, dielectric properties , and NDVI	-
[Notarnicola et al., 2006]	AirSAR + Landsat	95% row crop agriculture, 50% Corn and 45% soybeans	Dielectric properties, texture, NDVI, and roughness	
[Lakhankar et al., 2000]	SAR-1 + Landsat TM + ESTAR	winter wheat and a rangeland area	Texture, roughness, topography, vegetation optical depth, and NDVI	ESTAR image has been used to train and validate the network

[Ghedira et al., 2004]	ESTAR + Radarsat -1	mixed lan.d cover	Texture and optical depth	The overall accuracy increased from 56.2% to 77% after adding three texture bands to the network.
[Lakhankar et al., 2009]	SAR-1 + ESTAR + Landsat TM	mixed land cover	Soil texture, topography, and NDVI	ESTAR image was used to validate the method's results
[Bolten et al., 2003]	PALS Data (Radiometer channel)	vegetation cover, bare soil, pasture, crops, and trees	Surface roughness, texture, vegetation parameters, and bulk density	The results was provided using LH PALS channel
[Haider et al., 2004]	ERS2- SAR C-band	A mixed of vegetation and bare soil.	-	The correlation was measured between digital numbers and volumetric soil moisture
[Said et al., 2006]	ERS2-SAR C-band + LISS II	A mixed of vegetation and bare soil	Topography, vegetation, soil roughness	The calculated correlation was found for almost all vegetation classes and barren land

[Sprintsin et al., 2002]	ERS SAR	A desert	Surface roughness	
[Dubois et al., 1995]	SIR-C-band and airborne AIRSAR	Bare soil	Surface roughness	The algorithm is sensitive to the vegetation
[Said et al., 2008]	ERS-2 SAR	Bare soil, mixed vegetation and crops	Surface roughness, vegetation characteristics, sensor variables	-
[Carlson, 2007]	MODIS - Terra	Crop land, short vegetation, and agriculture fields	NDVI and T_s	The study area had different soil types given different correlations
[Wen et al., 2003]	TRMM/TMI	Sparse short-grass with some leaf area and about 0.03 m canopy heights.	T_s, leaf area index, and surface roughness	-
[Liou et al., 2001]	AMSR+ L-band SMOS	Bare soil and vegetated area	Viewing angle, frequency, observation mode, optical thickness and scattering albedo	The results were calculated using a 2-AMSR 6.9 GHz and 10.7 GHz frequency mode with zero noise

				imposed
[Blanchard et al., 1981]	ESMR	grassland watersheds	-	The soil moisture was measured for 23 cm depth
[Vecchia et al., 2007]	Brightness temperatures from L-band EMIRAD radiometer	A forest area includes a 5 cm litter layer	Dielectric constant	-

CHAPTER 3

DEVELOPMENT AND CHALLENGES OF APPLYING THE UNIVERSAL TRIANGLE RELATIONSHIP METHOD IN REMOTE SENSING APPLICATIONS*

ABSTRACT

The widely applied surface temperature–vegetation index (T_s –VI) triangle method is used in different remote sensing applications such as soil moisture estimation, soil surface evaporation, and soil surface evapotranspiration. Due to the method's wide application, it has been developed and several changes have been made to the method's mathematical concept. These changes have proved to produce better estimation results, but a few challenges have been encountered in applying these changes accurately. These challenges are presented by the ambiguity in identifying groups of pixels that outline the dry edge and the wet edge in the T_s-VI triangle space, and difficulty in choosing a suitable vegetation index in the T_s-VI triangle space that can produce the best results.

This study reviews the development and challenges of using the modified universal triangle method. Different applications of the method have been summarized and a conclusion is drawn based on the reviewed results.

---

* This paper is co-authored by Amer Ahmad and Yun Zhang and presented and accepted for publishing in *the 32nd Canadian Symposium on Remote Sensing and 14th Congress of the AQT*, June, 13-16, 2011, Sherbrooke, Québec, Canada. For the sake of clarity, this paper has been slightly edited.

It has been noticed that producing better estimation results using this method depends on the data distribution in the T_s-VI space and on the proposed algorithms of identifying the dry edge and the wet edge. On the other hand, lack of mathematical rules that can ensure applying these proposed changes properly might have an adverse effect on using this method effectively, and this can lead to misleading estimation results.

Keywords: Wet edge, Dry edge, T_s –VI space, Land Surface Temperature, Vegetation Index.

3.1 Introduction

Vegetation index is a unit less measurement of the amount of green vegetation in an area. It is an important parameter to distinguish a vegetation cover class from other classes. A widely used vegetation index is called Normalized Difference Vegetation Index (NDVI). NDVI was developed first for the Landsat satellite [Hardisky et al., 1983]; it has been widely used by researchers for years to determine the vegetated land cover of areas. In the meantime, another vegetation index was developed; i.e., the Enhanced Vegetation Index (EVI). It was first developed for Moderate Resolution Imaging Spectroradiometer (MODIS) satellite, and it has proven its effectiveness on dense vegetation areas.

One of the important methodologies that combines both land surface temperature and vegetation index was proposed by Carlson et al. [Carlson et al., 1997]; it is called Universal Triangle Relationship method or also called T_s-VI relationship. It was proposed based on an empirical-model that applies simple mathematical assumptions. Since proposing the method, it has been actively used in estimating results of different soil water applications, such as estimating evaporation and transpiration. The reason that makes this method widely used is its simplicity as it can be applied on any area that has both vegetation cover and bare soil without limitation.

3.2 Structure of T_s-VI Method

T_s-VI method is proposed based on interpreting the pixel values' information in two-dimensional space. The pixel values are projected into a two-dimensional scatterplot represented by T_s in the y-axis, vegetation index (VI) in the x-axis, and the variation in soil moisture is represented by the slope line of both T_s and VI. The trigonometric shape of the 2D plot is often results in a triangle shape [Price, 1990] or a trapezoid shape [Moran et al., 1994]. The location of each pixel in the T_s-VI plot is influenced by many factors based on the conditions of the research area and the accuracy of the pixel values.

According to the fractional vegetation cover, the T_s-VI space is divided into three main areas: an upper left area (identified by the red ellipsoid), middle area (identified by the orange ellipsoid), and lower right area (identified by the green ellipsoid), as shown in

Figure (3.1). The pixels that come from dry areas or bare soil should be located within the red ellipsoid, the pixels that come from a mix of bare soil and vegetation should be located in the orange middle zone ellipsoid, and the pixels that come from wet areas such as water bodies or vegetation areas should be drawn at the bottom right of the triangle and within the green ellipsoid. The amount of transpiration increases when the pixels are moving from wet areas to dry areas unlike the amount of evaporation that goes in the opposite direction. Soil moisture is represented by the graduated slope of the triangle; it increases from 0 (which means a very wet area) to 1 (which means a very dry area).

After plotting the relationship between pixels' temperature and the area's vegetation index, a best fit line for the whole pixel values will be drawn. The best fit line for the whole pixels in the plot is called "the dry edge"; it mostly contains pixels that have a high surface temperature and low vegetation index. The bottom horizontal line that extends parallel to the x-axis called "the wet edge", which represents the pixels that are coming from wet areas with low surface temperature. After identifying the edges, TVDI equation below, equation (3.1), should be applied to calculate the soil moisture index.

$$TVDI = \frac{T_s - T_{s\,\min}}{a + bNDVI - T_{s\,\min}} \qquad (3.1)$$

Where T_s = surface temperature for a given pixel in the plot, $T_{s\,\min}$ = linear equation of the fit line at the wet edge area, *a* and *b* are constant parameters resulting from a linear fit to data. The TVDI equation is a mathematical representation for the difference between the distance (A) and distance (B) shown in the figure below. Distance A represents the difference between any pixel value located within the T_s-VI plot and the minimum value of T_s in the plot; (B) represents the difference between the best fit line equation of the

overall pixels and the minimum T_s value in the plot. TVDI values should range between 0 (for wet areas) to1 (for dry areas).

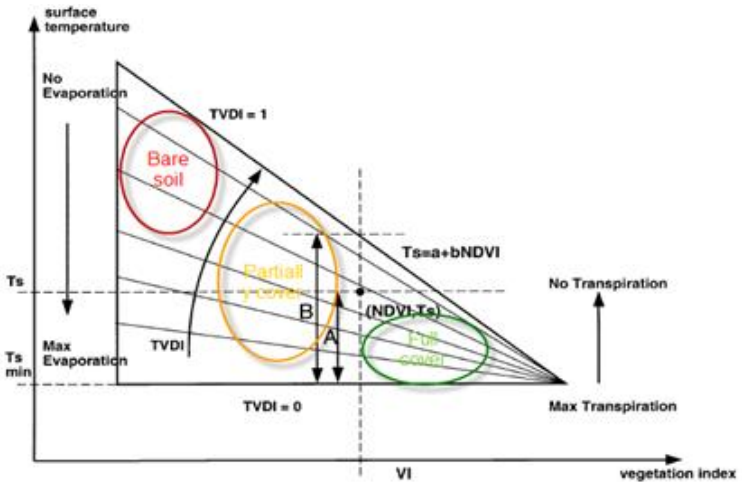

Figure 3.1 The original concept of the T_s-VI method showing pixels distribution in the space, modified after [Sandholt, 2002]. Red ellipsoid represents pixels that come from hot areas, orange ellipse represents pixels that come from a mixed of wet and dry areas, green ellipse represents pixels that come from wet areas. TVDI increase relatively with increase of T_s and decrease VI.

3.3 Current Applications of T_s-VI Method

The method is widely applicable in any area that has a combination of vegetated soil and bare soil. The two main input parameters of the method are the surface temperature and the fraction of vegetation index. Therefore, researchers use different approaches with remote sensing data to calculate the method's input parameters, and these different approaches lead to different estimation results. Many researchers have utilized the triangle method. Gilles et al. [1997] used airborn multispectral radiometer data to extract

the method's two main parameters. Nishida et al. [2003] used the principles of triangle method to estimate the evaporation fraction that is expressed as a ratio of actual evapotranspiration (ET) to the available energy using NOAA/AVHRR data. Jiang and Islam [2003] proposed a simple scheme for the distribution of surface latent heat flux based on an interpretation of the triangle method using vegetation index data and radiometric surface temperature. Wang et al. [2006] integrated a thermal inertial method with triangle method to develop a modified day-night surface temperature with NDVI. They plotted the two parameters in a triangular space using MODIS Aqua and MODIS Terra data to estimate the evapotranspiration. Hassan et al. [2007] proposed a new wetness index using terrain-corrected surface temperature and normalized difference vegetation index derived from MODIS products based on the principles of the triangle method. Sun et al. [2008] applied the triangle method by extracting surface temperature from Land sat TM to estimate soil moisture information. Sisten et al. [2008] applied the original principles of the triangle method using MSG-SEVIRI data to calculate each of T_s and NDVI, and then they plotted the two parameters in one space to estimate the air temperature.

Some researchers used MODIS surface reflectance and use MODIS surface reflectance bands to calculate the VI as we did in this research. Yao et al. [2011] applied the simplified principles of the triangle method using Albedo- vegetation index space to determine the Priestley–Taylor parameter for estimating evaporative fraction and evapotranspiration in arid and semi-arid regions using MODIS data [Yao et al, 2011]. Lately, Nieto et al. [2011] have estimated air temperature using thermal infrared and

optical wavelength information by finding a relationship between the observed land surface temperature (T_s) and a spectral vegetation index (NDVI).

Some of these presented researchers have neglected the influence of either the atmospheric conditions or the influence of topographic changes. Correcting both effects might be challenging, but they both substantially influence estimation of soil water applications.

3.4 Challenges of Applying T_s-VI Method

An important challenge that needs to be considered in remote sensing data before applying the universal relationship method is that the data should be atmospherically and topographically corrected by having free cloud-cover, free atmospheric gases or vapor, and free solar illumination. This method mainly depends on the imagery's pixel values; the more accurate the pixel values are, the better the expected results. Another challenge in of applying this method is represented by choosing the right selection of pixels that forms the wet edge or the dry edge. For instance, when the method was proposed first, choosing the dry edge was simply represented by the best fit line of the pixels that have the highest surface temperature in the T_s-VI space. Similarly for the wet edge, it was easily represented by a horizontal line at the minimum value of surface temperature. However, as the method has evolved, a few changes have arisen in identifying both the wet and the dry edges. These changes are resulted from the flexible rules of outlining

both edges; such as using different algorithms to identify the dry edge considering pixels location in the T_s-VI scatter plot and pixels tendency to form a linear regression line.

There are no pre-defined mathematical rules to identifying the dry or wet edge; it is represented by a best fit line for a group of pixels located at the dry or wet edge. The pixels that form a wet or a dry edge are selected based on how related they are to each other with respect to their location in the T_s-VI space.

Another challenge to be considered is that when selecting a group of pixels to identify both edges, some pixels that are located outside the selection will be neglected and will not be represented in the equation of the best fit line. For example, the pixels that have a similar trend (located at a fairly close distance) will be represented in the equation of the best fit line as the dry edge pixels; however, the pixels that are dispersed or deviated from the trend, either for having extremely high or low T_s or extremely high or low VI will be left out and will not be represented in the line's equation, see Figure 3.2.

Another uncertainty that can be added to the method's applicability is that different vegetation indexes can be used to draw the T_s-VI space, and a vegetation index can produce different results at different areas' conditions. Therefore, it is not easy to choose the right vegetation index that can deliver the best estimation results. In addition, MODIS, Landsat, or AVHRR are the most widely used optical data in this method; these data normally have a coarse resolution that might be difficult to accurately identify the wet or the dry areas in the image since some pixels can be splitted in between wet and dry areas, but the pixel value can only be represented in one position in the T_s-VI space.

Lastly, current researches have been using low resolution imagery to estimate soil moisture distribution on large scale areas. However, if we were dealing with high resolution image, we expect the process to be more complex as more pixels will be plotted in the T_s-VI space.

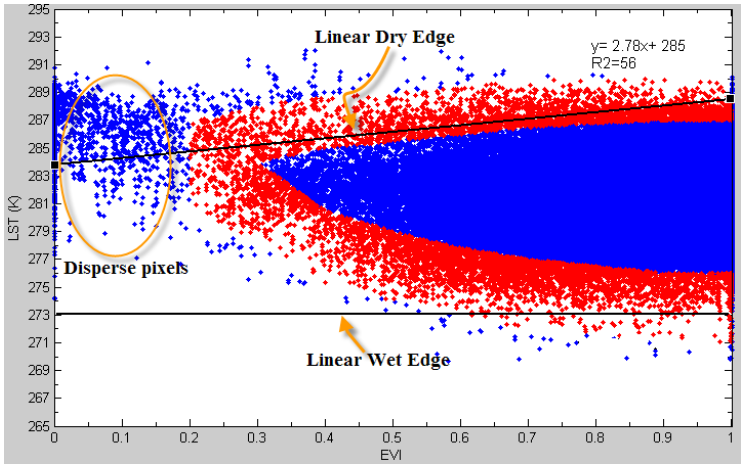

Figure 3.2 Example for pixels distribution in the T_s-VI Space. The plot shows that there is inaccuracy in choosing the number of pixels that identifies both of the dry or the wet edge. Pixels located outside the trend of dry and wet edge are neglected and not considered in the equation of best fit line.

3.6 Conclusion

The universal triangle method is widely used in different remote sensing applications due to its ease of use, flexibility, and applicability in different areas. However, a few challenges can lead to uncertainty in applying the method properly such as:

- Not all pixels drawn in the T_s-VI space are represented in the equation of best fit line of the dry and the wet edges. Some pixels might have a higher or lower

surface temperature that will tend to exclude them from the selected group of pixels that identify the line of each edge.

- As the method has evolved, no mathematical rules have been set to identify the pixels in the dry and the wet edges. It all depends on the proposed algorithm that identifies the wet edge and the dry edge.
- It is difficult to identify a suitable vegetation parameter to be used in the T_s-VI space. Some vegetation indexes might give good results in one area, but they might deliver poor results in a different area. Therefore, defining the triangle space depends on the vegetation parameter used.
- Optical satellite data such as MODIS or AVHRR are the most widely used information in this method; however, they do not deliver the best estimation results compared with using radiometric data or radar data. These less accurate results might be due to the coarse resolution of the optical satellites used as capturing the warm or the dry edge might be difficult if the pixel value is fragmented in both warm and wet areas.

Acknowledgments

The author would like to thanks Mr. Titus Tienaah, A graduated MSc.E. student in the department of Geomatics Engineering at the University of New Brunswick for his comments and feedback to make this paper better.

References

Gillies, R. R., T. N. Carlson, J. Cui, W. P. Kustas, and K. P. Humes (1997). "Verification of the triangle method for obtaining surface soil water content and energy fluxes from remote measurements of Normalized Difference Vegetation Index (NDVI) and surface radiant temperature." *International Journal of Remote Sensing,* Vol.18, pp.3145-3166.

Hardisky, M. A., Klemas, V., and Smart, R. M. (1983). "The influences of soil salinity, growth form, and leaf moisture on the spectral reflectance of Spartina alterniflora canopies". *Photogrammetric Engineering and Remote Sensing,* Vol.49, pp.77– 83.

Hassan, Q. K., C. P. -. Bourque, F. Meng, and R. M. Cox (2007). "A wetness index using terrain-corrected surface temperature and normalized difference vegetation index derived from standard MODIS products: An evaluation of its use in a humid forest-dominated region of eastern Canada." *Sensors Journal,* Vol.7, pp.2028-2048.

Jiang, L., and S. Islam (2003). "An intercomparison of regional latent heat flux estimation using remote sensing data." *Journal of Remote Sensing,* Vol.24, No.11, pp.2221-2236.

Moran, M. S., T. Clarke, W. P. Kustas, M. Weltz, and S. A. Amer (1994). "Evaluation of hydrologic parameters in a semiarid rangeland using remotely sensed spectral data." *Water Resources Research,* Vol.30, No.5, pp.1287-1297.

Nieto, H., I. Sandholt , I. Aguado , E. Chuvieco, and S. Stisen (2011). "Air temperature estimation with MSG-SEVIRI data: Calibration and validation of the TVX algorithm for the Iberian Peninsula." *Remote Sensing of Environment,* Vol.115, pp.107-116.

Nishida, K., R. R. Nemani, S. W. Running, and J. M. Glassy (2003). "An operational remote sensing algorithm of land surface evaporation." Vol.108(D9), pp.4270.

Price, J. C. (1990). "Using spatial context in satellite data to infer regional scale evapotranspiration." *IEEE Transactions on Geoscience and Remote Sensing Journal,* Vol.28, pp.940-948.

Sandholt, I., K. Rasmussen, and J. Andersen (2002). "A simple interpretation of the surface temperature/ vegetation index space for assessment of surface moisture status." *Remote Sensing of Environment,* Vol.79, pp.213-224.

Stisen, S., I. Sandholt, A. Nørgaard, R. Fensholt, and K. H. Jensen (2008). "Combining the triangle method with thermal inertia to estimate regional evapotranspiration-Applied to MSG/SEVIRI data in the Senegal River basin." *Remote Sensing of Environment,* Vol.112, pp.1242-1255.

Sun, Q., J. Tan, and S. Chen (2008). "Estimation of soil conditions with Landsat TM in Guangzhou." *Proce. of SPIE,* Vol.7145,.

Tang, R., Z. Li, and B. Tang (2010). "An application of the T_s–VI triangle method with enhanced edges determination for evapotranspiration estimation from MODIS data in arid and semi-arid regions: Implementation and validation." *Remote Sensing of Environment,* Vol.114, pp.540-551.

Wang, K., Z. Li, and M. Cribb (2006). "Estimation of evaporative fraction from a combination of day and night land surface temperatures and NDVI: A new method to determine the Priestley-Taylor parameter." *Remote Sensing of Environment,* Vol.102, pp.193-305.

Yao, Y., Q. Qin, A. Ghulam, S. Liu, S. Zhao, Z. Xu, and H. Dong (2011). "Simple method to determine the Priestley–Taylor parameter for evapotranspiration estimation using Albedo-VI triangular space from MODIS data." *Journal of Applied Remote Sensing,* Vol.5, pp.053505-1-053505-16.

CHAPTER 4

COMPARISON OF SOIL-MOISTURE INDEX CALCULATIONS BASED ON SUN-ILLUMINATION CORRECTED AND UNCORRECTED LAND SURFACE TEMPERATURE AND VEGETATION INDICES GENERATED FROM MODIS DATA*

ABSTRACT

Optical satellite imagery is considered a valuable source of data for estimating soil-moisture characteristics in complex landscapes. However, these data are regularly influenced by prevailing atmospheric conditions and variation in topographic relief; significant variation in any one of these variables can degrade image information. To correct the sun-illumination effect produced by variable terrain, a great number of scientific publications have proposed various approaches. None of these approaches, however, have been used to assess the effectiveness of these corrections in describing ground-surface biophysical conditions and their distributions, including those associated with soil moisture.

This paper proposes an integrated approach to address the influence of solar illumination on the calculation of Temperature Vegetation Dryness Index (TVDI; an index of soil dryness). The integrated approach includes an application of a pre-processing step based on the C-correction method and a modified universal triangle

---

*This paper is co-authored by Amer Ahmad, Yun Zhang, and Charles Bourque; it will be submitted for publication in the Journal *Remote Sensing of Environment*. For the sake of clarity, the paper has been slightly edited.

method to estimate TVDI from 8-day composites of land surface temperature (T_s) and vegetation index (VI) generated from emission and reflectance data acquired with the Moderate Resolution Imaging Spectroradiometer (MODIS) sensor on the Terra satellite. Modification to the T_s-VI triangular relationship portrays the wet and dry edges of the relationship as linearly varying variables, both before and after correction. TVDI-calculation sensitivity to the choice of VI, i.e., Enhanced Vegetation Index (EVI) or the more commonly used Normalized Difference Vegetation Index (NDVI), is examined.

Based on both visual and statistical comparisons of distributions of derived TVDI-values and mapped wetland, TVDI-values are shown to ameliorate when terrain-induced illumination effects are removed. The study also shows EVI, when used in the definition of the T_s-VI solution space, produces better results than when NDVI is used.

Keywords: Lambertian assumption, Solar-illumination correction, Soil moisture, T_s-VI space, TVDI, Vegetation index.

4.1 Introduction

Over the past decade, environmental changes have impacted human life dramatically. These changes have led researchers to investigate new approaches in environmental monitoring using various remote sensing (RS) techniques. One such area of active research concerns the monitoring of soil moisture from space-borne sensors. Intervallic

monitoring of the hydrological cycle is essential to avoid unexpected outcomes in regional soil-water supply. With respect to the water balance, soil moisture influences the rate of evapotranspiration, groundwater recharge, and surface-water runoff [Haibin et al., 2007]. Aside from precipitation levels and wind, soil moisture is regularly influenced by changes in topography, resulting in re-distribution of precipitated water, and illumination angle (energy input). For instance, high-elevation areas with high ambient temperatures and high drainage and isolation characteristics tend to be less moist than low-elevation, shady areas with low ambient temperatures.

From a RS-data perspective, optical data are influenced by many external factors, such as ground-surface roughness, atmospheric forcing, land cover, and image-acquisition times, as well as internal conditions related to the configuration and the physical properties of the sensor [Sandholt et al., 2002].

Generally, bright spots in RS-images that correspond to flat terrain (assuming no change in satellite incidence angle) are representative of hot, dry areas. This correlation arises mainly because dry soils tend to (i) reflect more solar radiation, as a result of high surface albedo (~0.35), and (ii) support lower levels of evapotranspiration and, therefore, cooling, as compared to wet soils with a low surface albedo (~0.08) and increased energy absorption and evapotranspiration. Surface albedo is defined as the ratio of the radiant flux reflected from the earth's surface to the incident energy flux [Sato and Katsushi, 1994]. The situation, however, becomes considerably more complicated when dealing with areas in variable terrain. Variation in topography causes elements of the terrain (pixels) to have different orientations to the sun. This variation causes land-surface

elements facing into the sun to appear bright and land-surface elements facing away from the sun to appear dark, as a result of self-shading. Consequently, confusion might arise as to whether an area is illuminated because of its orientation to the sun or because of its inherent moisture status. Clearly, accurate interpretation of a pixel's soil-moisture status requires that terrain-induced illumination effects are removed prior mapping soil-moisture-related indicators.

4.1.1 Methods Available for Correcting Sun-Illumination Effects

Terrain-enhanced surface-illumination effects in RS images have been widely recognized by researchers as being problematic when interpreting unprocessed optical images [Leprieur et al., 1988; Teillet et al., 1986; Thomson and Jones, 1990]. Several approaches have been proposed to solve this problem. Because the error is primarily associated with sun position (i.e., illumination angle) and ground elevations, the error can be corrected by accounting for sun-earth geometry and digital terrain elevations (extracted from digital elevation models, DEMs), from which slope, slope orientation (aspect), solar illumination angle, terrain configuration and view factors, and other terrain and sun angle-related variables can be derived. In general, to correct terrain-induced sun-illumination effects in optical imagery, two basic sets of assumptions are employed: (i)

Lambertian, and (ii) non-Lambertian [Kobyashi and Sanga-Nogie, 2003; Meyer et al., 1993].

Lambertian - The Lambertian model was first proposed to explain the response of surface irradiance in relation to ground-surface configuration. It is based on assumptions that (i) the ground surface receiving incoming solar energy is flat, (ii) there is a constant flux of solar energy to the earth's surface, (iii) there is an equal amount of energy reflected in all directions (isotropic reflection), and (iv) the correction is wavelength independent [Meyer et al., 1993; Law and Nichol, 2010]. Examples of corrections based on Lambertian assumptions are the cosine, modified-cosine, and C-correction [Liu et al., 2007].

Non-Lambertian - The non-Lambertian model was proposed to improve the manner in which surface irradiance is modeled to interact with the earth's surface. The non-Lambertian model specifies that (i) the ground surface receiving solar energy is irregular, (ii) the energy is reflected unequally in all directions (anisotropic reflection), and (iii) the correction is wavelength dependent. Examples of corrections based on non-Lambertian assumptions are the Minnaert and statistical correction [Liu et al., 2007]. Techniques based on either set of assumptions rely on the accessibility of the same solar angle-related inputs.

Both models yield acceptable results, although they may over- or under-estimate the error for individual pixels. For the most part, the models neutralize image error by

increasing mean pixel values of areas located in the shady portion of the image and decreasing pixel values of areas in the sunny portion.

Different theoretical approaches have been proposed to estimate the sun-position variables in order to calculate a sun-illumination-correction factor to correct optical images. However, none of these approaches have been evaluated as to their suitability in RS-based environmental applications. Each approach has its own set of advantages, disadvantages, and application requirements. Sun-illumination image correction has been widely used [Twele et al., 2007; Zhang et al., 2011] but only a few of the available methods are recommended, one of which is the C-correction [Kobayashi et al., 1993] despite its tendency to over-correct image-areas illuminated from high incidence angles (Liu et al., 2007].

4.1.2 Article Objectives

Primary objective of this research is to examine the role terrain-induced solar-illumination effects may have on the Temperature Vegetation Dryness Index (TVDI), an index of soil dryness. The research also investigates (i) the effectiveness of using EVI (Enhanced Vegetation Index) as a substitute for the less sensitive (Yang, Wu, Shi, & Yan, 2008; Huete, Didan, Miura, Rodriguez, Gao, & Ferreira, 2002) and more commonly used NDVI (Normalized Difference Vegetation Index) in the triangular definition of land-surface temperature-vs.-vegetation index (T_s-VI) relationship, from which TVDI is

derived, and (ii) the usefulness of a sloped (non-constant) wet edge in the definition of T_s-VI space.

4.2 Methods and Materials

4.2.1 Study Area

The study area is 105 000 km^2, covering about 75% of the Province of New Brunswick (NB) in Atlantic Canada (see Figure 4.1). The area is dominated by over 80% forests. Elevations in the study area ranges from about 0-834 m above mean sea level (AMSL), with the higher elevations in the north and northeast-central portion of the study area. The climate is characterized as cool-moist, with an annual precipitation ranging from 1000-1500 mm, the heaviest normally falling during autumn and at the beginning of the snow-accumulation season.

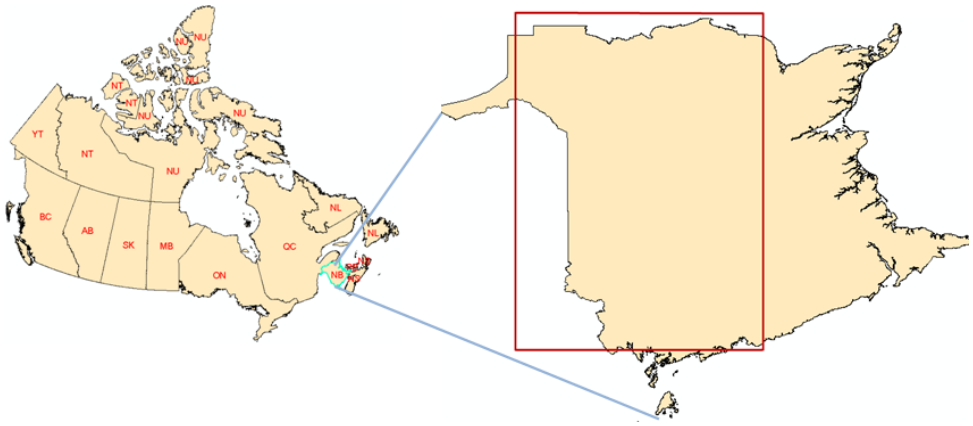

Figure 4.1 The upper left map shows the map of Canada and the location of the province of New Brunswick (NB) with respect to Canada. The map of NB shows the location of the study area (red rectangle); the area includes portions of southeastern Quebec and northeastern Maine, USA.

4.2.2 Data Employed

Study-input data included Moderate Resolution Imaging Spectroradiometer (MODIS)-based (i) 8-day composites of land surface temperature (T_s; Band 31; MOD11A1 product at 1-km resolution) and surface reflectance of the red (R), near infrared (NIR), and blue (B) bands (SR; MOD09 product at 500-m resolution) for 01 May and 30 September, 2003, acquired from the Land Processes Distributed Active Archive Center (LP DAAC; https://lpdaac.usgs.gov/lpdaac/get_data/data_pool, last accessed on May 10, 2011), and (ii) MODIS-based Geolocation data (MOD03; solar azimuth and zenith angles) acquired from the Level 1 and Atmosphere Archive and Distribution System website (LAADS; http://ladsweb.nascom.nasa.gov, last accessed on May 10, 2011). All images were geo-referenced and cropped to the bounds of the study area (Figure 4.1) in ENVI™. SR-images were subsequently re-sampled to 1-km resolution. A Digital Elevation Model (DEM) of the study area was acquired from the Canadian GeoBase database [Canadian Geobase Data, 2011] with a map scale of 1:50,000 and 0.75 arc-second resolution. The DEM was later re-sampled to 17-arc minutes (see Figure 4.2).

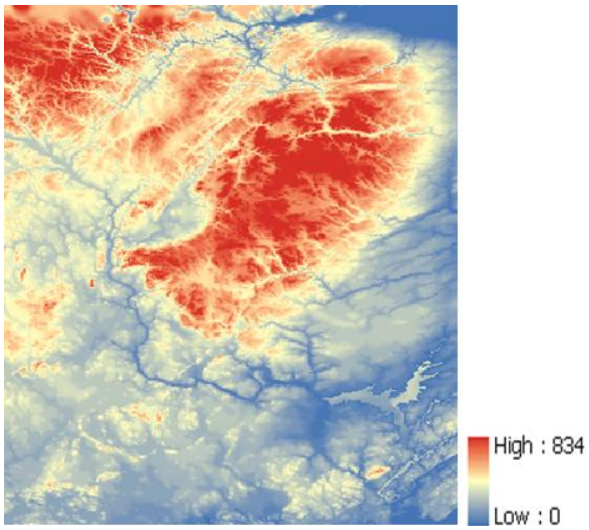

Figure 4.2 Digital elevation model used in this study. Elevations are in Metres above mean sea level

4.2.3 Data Processing

The study proceeds with (i) calculating T_s (in K), NDVI, and EVI (non-dimensional) ***without*** and ***with*** correction to emission and SR bands for sun-illumination effects; (ii) generating triangular T_s-VI plots [Carlson, 2007] using both uncorrected and corrected T_s and one of two vegetation indices, i.e., NDVI or EVI; and (iii) comparing TVDI (non-dimensional) generated from the series of T_s-VI plots. Because EVI is more sensitive to differences in vegetation density and terrain-surface orientation than is NDVI [Matsushita et al., 2007], we extend our work to include an examination of the choice of vegetation index (i.e., NDVI or EVI, before and after correction) in constructing T_s-VI plots and TDVI determination. Generation of correction factors for emission and SR band-specific images (used in the computation of T_s, NDVI and EVI) involves pre-processing MODIS-

based sun-position data and assessing terrain-induced relative illumination, expressed here as a value between -1.0 (representing low illumination) and 1.0 (high illumination).

4.2.3.1 Image Correction for Sun-illumination Effects

The C-correction was first proposed by Teillet [Teillet, 1986] and named as such by Meyer et al. [Meyer et al., 1993]. This method aims to remove pixel-illumination dependency on terrain characteristics by de-correlating the relationship between pixel-reflectance (digital number) and the illumination-scale factor (IL; see Figure 3) [Tan et al., 2010] estimated with

$$IL = \cos Z = \cos\theta_p \cos\theta_z + \sin\theta_p \sin\theta_z \cos\left(\phi_a - \phi_o\right) \quad (4.1)$$

where Z is the incident angle; ϕ_a and θ_z are solar azimuth and zenith angle obtained from MOD03-products; and θ_p and ϕ_o are slope and slope-orientation angles calculated with the re-sampled DEM (see Figure 4.2).

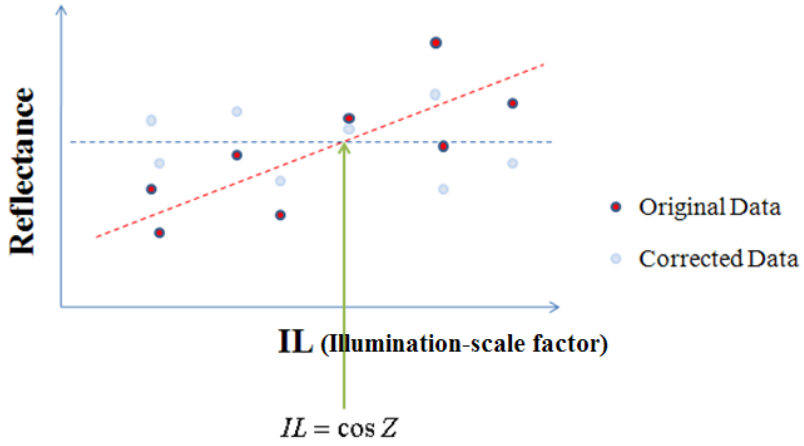

Figure 4.3 Pixel-reflectance dependency on the illumination-scale factor before (red dashed line; positive correlation) and after solar-illumination correction (blue dashed line; zero correlation). Data transformations are based on procedures outlined in Masek et al [after Masek et al., 2010].

C-correction of land-surface images (i.e., emission and SR bands) is based on the following set of equations:

$$L_T = b_k + m_k IL \tag{4.2}$$

where L_T is the radiance observed over sloped terrain (**uncorrected** image value), b_k and m_k are equation coefficients determined by least squares regression of pixel radiance values (L_T) and IL (red dashed line; Figure 4.3), c_k is the C-correction coefficient and is given as a ratio of regression coefficients b_k and m_k, i.e., $c_k = \frac{b_k}{m_k}$; k signifies illumination-dependency on reflectance-emission bands. De-correlation of the original illumination data (closed red symbols, in Figure 4.3) is based on the mathematical operation,

$$L_H = L_T \left(\frac{\cos\theta_z + c_k}{IL + c_k} \right) \tag{4.3}$$

where L_H is the expected radiance on a horizontal surface and represents the **corrected** image-pixel value (open light-blue symbols; Figure 3). Calculation of NDVI and EVI are based on expressions that use R, NIR, and B bands before and after correction. Correction to T_s follows with a correction to Band 31 of MOD11A1-products.

4.2.3.2 T_s-VI Space Definition

The T_s-VI method was first proposed by Carlson et al. [Carlson, 1997]. It generates a two-dimensional surface defined by T_s (y-axis, Figure 4.4) and a VI of a given area (typically, NDVI; x-axis, Figure 4.4) and used to estimate TVDI. The method assumes that the shape of the relationship is either triangular (as illustrated in Fig 4.4) or a slightly-truncated trapezoid. In contrast to the original triangular approach (see Figure 4.4), in our study we permit both dry and wet edges to vary as a function of VI (specified here either as NDVI or EVI). Their expressions are developed from linear regression applied to T_s and VI data representative of either the lower boundary of the T_s-VI space and, therefore, the "wet edge" of the relationship, where TVDI=0.0, or the upper boundary or "dry edge", where TVDI=1.0 (see Figure 4. 4).

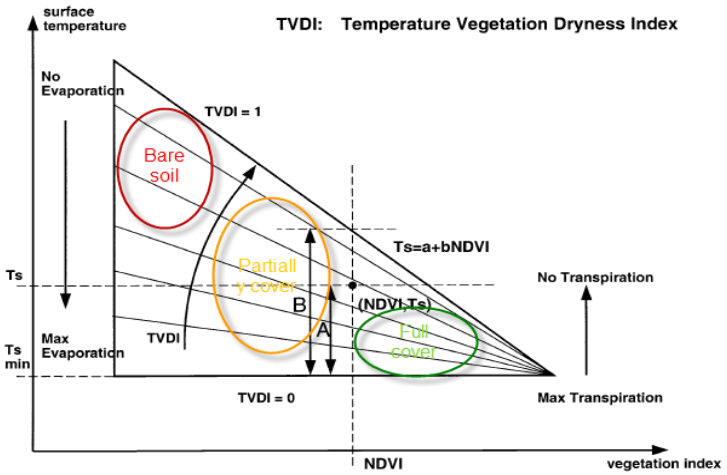

Figure 4.4 Schematic of T_s-VI relationship as originally proposed and illustrated in Sandholt et al., modified after Sandholt et al. [2002]. The schematic shows pixel distribution across the triangular space; (i) the red ellipse identifies the space where pixels are representative of dry, non-vegetated to sparsely-vegetated areas; (ii) the orange ellipse, dry to sub-humid, moderately-vegetated areas; and (iii) the green ellipse, sub-humid to humid, densely-vegetated areas

Estimation of TVDI is based on a normalization of T_s , i.e.,

$$TVDI = \frac{Ts - Ts_{\min}}{Ts_{\max} - Ts_{\min}} \qquad (4.4)$$

where $T_{s\,min}$ and $T_{s\,max}$ represent the linearly-changing (sloped) wet and dry edges of the T_s-VI apace (see Figure 4.4). Figure 4.5 summarizes the steps taken to estimate TVDI from various perspectives, specifically (i) without correction to emission and SR bands (and T_s, NDVI, and EVI), and (ii) with implementation of either NDVI or EVI in the T_s-VI relationship.

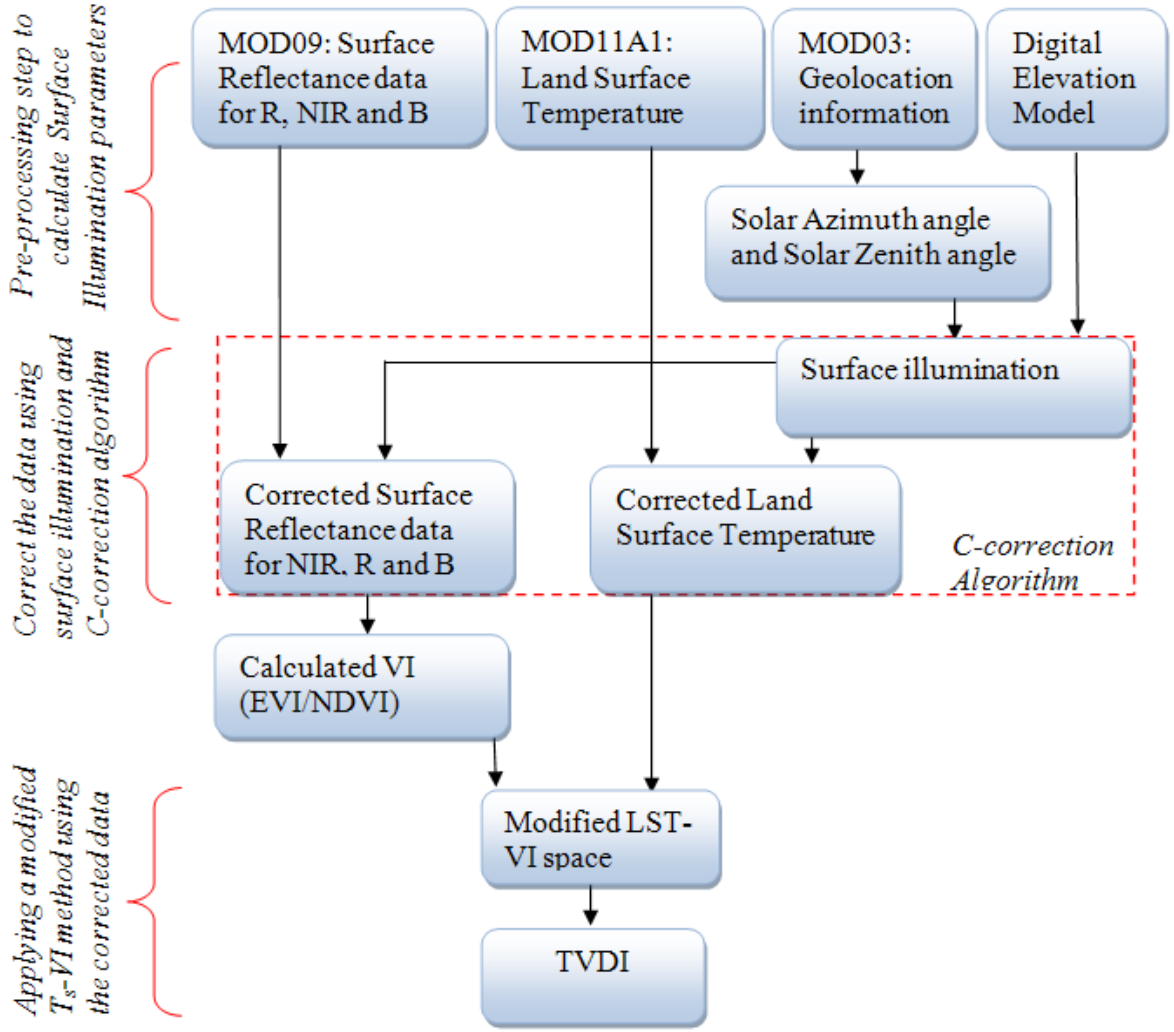

Figure 4.5 A Flow diagram showing the steps taken to generate estimates of TVDI from illumination-corrected data.

4.3 Results Discussion

4.3.1 Effectiveness of Data Correction

First, the result of utilizing the correction method in this approach, C-correction method, needs to be investigated to confirm that it works effectively with the MODIS data. To determine how effective the applied C-correction method in removing sun-illumination error from the data employed, two evaluation approaches are analyzed from the obtained results: Visual evaluation and statistical analysis.

The results analyses are conducted on the data before and after applying the illumination correction. Statistical analysis is conducted to calculate the pixels' mean value (μ) and pixels' standard deviation (σ). The standard deviation is considered as a measure of deviation of pixel-values from the average value. The mean value of the pixels located at the shady spots should increase while the mean value for pixels located on the sunny spots should decrease. Furthermore, the corrected data should have a lower standard deviation compared with uncorrected data.

Another statistical analysis is applied, which is the linear regression analysis. A statistical method is applied using a scatter plot to draw the relationship between the illumination surface and each MODIS spectral band used before and after the correction. The higher the correlation is, the more illumination is found in the pixel information and vice versa. Therefore, de-correlating the relationship between the surface illumination

and the corrected data indicates that the error is reduced [Masek et al., 2010]. Below is a technical description for each processing step applied in this approach.

4.3.1.1 Visual Evaluation

Before implementing the correction, it was noticed that the gray-scale of the non-corrected images seemed to have a high contrast; some areas seemed too bright and some spots seemed to be too dark. After the correction was implemented, the contrast between both of the dark and bright spots is reduced and the corrected images seem to have less colour variation with higher pixels' homogeneity (see Figures 4.6 and 4.7); reducing the image contrast is also related to the pixels' response to the correction by changing their bright colour to dark and the dark colour to bright. However, a noticeable change is found after correcting some pixels that are located in shady areas, they seem to be too bright after the correction. This new bright areas can be interpreted as that they were overcorrected, which is the disadvantage of the C-correction algorithm. On the other hand, the correction results between both of May and September dataset were different. For instance, May dataset is changed significantly after applying the correction and that means that the data is more responded to the correction and better corrected compared with September dataset. In the meantime, there is not much visual difference between the SR bands before and after the correction when September dataset is processed (see Figure 4.6). These visual results are in accord with the statistical analysis that is implemented on the data before and after applying the correction as the differences between the calculated

statistics using May dataset is more significant than the difference using September dataset; more discussion will be in the next section (section 4.3.1.2).

4.3.1.2. Statistical Analysis

The calculated statistics from T_s images after implementing the correction in both data dates show that the mean value remains relatively close to the mean value before the correction and the standard deviation is lowered significantly (see Table 4.1); the mean value for the three SR bands is not much different from that of the images before correction and the standard deviation is lowered using May 01 dataset. Similarly, the standard deviation is decreased in both of the calculated EVI and NDVI when the data was corrected (Table 4.3). Nevertheless, it has been noticed that the standard deviations' decrease using the May 01 dataset is more significant that the standard deviation's decrease using the September 30 dataset; and that interprets the significant difference of visual results in both data dates.

A linear regression analysis was applied in the T_s-VI space to calculate the main three statistical parameters: **a**, **b** and $\mathbf{R^2}$. Where **a** and **b** are the linear fit parameters and $\mathbf{R^2}$ is the correlation coefficient for the linear fit for each of the dry edge, wet edge, and the overall fit. Judging based on R^2, the results of both dataset dates show that correlation analysis conducted between the illumination-surface factor and T_s is significantly

decreased; similarly when comparing the correlation between illumination -surface factor and surface reflectance of R and NIR bands in May dataset (see Tables 4.2).

From both the visual and statistical analysis we can conclude that, in general, the applied approach was able to reduce the illumination error. However, the approach was not able to remove all the illuminated or dark spots in the images, and that can be clearly seen in the SR bands using the September dataset.

Table 4.1 Mean (μ) and standard deviation (σ) for the dataset before and after correction.

Band	**Original image**		**Corrected image**		**Data Date**
	μ	σ	μ	σ	
T_s- Band 31	282.4	39.2	283.2	36.8	May 01, 2003
	233.84	106.43	210.1	95.65	Sept. 30, 2003
SR- Red Band	0.07	0.089	0.065	0.03	May 01, 2003
	0.097	0.108	0.087	0.096	Sept. 30, 2003
SR- NIR Band	0.216	0.134	0.215	0.053	May 01, 2003
	0.276	0.103	0.275	0.10	Sept. 30, 2003
SR- Blue Band	0.036	0.05	0.033	0.018	May 01, 2003
	0.089	0.115	0.077	0.099	Sept. 30, 2003

Table 4.2 Statistical parameters before and after correction. The statistical parameters are calculated for the linear fit of the overall pixels in the scatter plot (aoverall, boverall and R^2 overall), the linear fit parameters for pixels of the wet edge in the scatter plot (**a**wet, **b**wet and R^2 wet) and the linear fit parameters for pixels of the dry edge in the scatter plot (**a**dry, **b**dry and R^2 dry).

	Before correction				**After correction**				Statistical Parameter	Data date in 2003
Bands	T_s	SR- R	SR- NIR	SR- B	T_s	SR-R	SR- NIR	SR- B		
Illumination-surface factor	0.57 0.39	-0.003 0.011	-0.002 0.003	-0.002 0.013	-0.2 0.092	-0.003 0.01	-0.002 0.003	-0.002 0.01	$a_{overall}$	May 01 Sept.30
	288 282	0.064 0.095	0.22 0.28	0.033 0.086	288 282	0.065 0.085	0.216 0.28	0.034 0.075	$b_{overall}$	May 01 Sept.30
	10.4 8	7 6.1	2 1.8	6.7 6.5	3.6 2.1	6.8 6	1.13 1.7	6.5 6.3	$R^2_{overall}$ (%)	May 01 Sept.30
NDVI	4.66 1.35	-	-	-	5.27 1.5	-	-	-	$a_{overall}$	May 01 Sept.30
	285 282	-	-	-	285 281	-	-	-	$b_{overall}$	May 01 Sept.30
	17.6 5.5	-	-	-	19.6 6.8	-	-	-	$R^2_{overall}$ (%)	May 01 Sept.30

	-	-	-	-	5.38	-	-	-	a_{dry}	May 01
	-	-	-	-	2.93	-	-	-		Sept.30
	-	-	-	-	290	-	-	-	b_{dry}	May 01
	-	-	-	-	286	-	-	-		Sept.30
	-	-	-	-	33.4	-	-	-	R^2_{dry} (%)	May 01
	-	-	-	-	46.8	-	-	-		Sept.30
	-	-	-	-	-2.83	-	-	-	a_{wet}	May 01
	-	-	-	-	-8.41	-	-	-		Sept.30
	-	-	-	-	281	-	-	-	b_{wet}	May 01
	-	-	-	-	280	-	-	-		Sept.30
	-	-	-	-	34	-	-	-	R^2_{wet} (%)	May 01
	-	-	-	-	53	-	-	-		Sept.30
EVI	2.24	-	-	-	2.61	-	-	-	$a_{overall}$	May 01
	2.1				-0.02					Sept.30
	286	-	-	-	286	-	-	-	$b_{overall}$	May 01
	281				282					Sept.30
	12.3	-	-	-	14	-	-	-	$R^2_{overall}$ (%)	May 01
	8				8.1					Sept.30

	3.12 -2.12 290 288 55.4 2.8	-	-	-	4.95 2.78 290 285 72 56	-	-	-	a_{dry} b_{dry} R^2_{dry} (%)	May 01 Sept.30 May 01 Sept.30 May 01 Sept.30
	-7.51 1.16 287 276 80 5.3	-	-	-	-7.08 -9.55 286 283 72.4 76	-	-	-	a_{wet} b_{wet} R^2_{wet} (%)	May 01 Sept.30 May 01 Sept.30 May 01 Sept.30

4.3.2 Analysis of Soil Moisture Information Results

A visual and statistical analysis is implemented on the soil moisture results by comparing the estimation results before and after the illumination is corrected to determine the followings:

1. How effective the correction was in improving the estimated results?

2. How effective were the two changes that were made to the original concept of T_s-EVI space: Using EVI instead of the NDVI and assuming that the wet edge is changing linearly rather than being a steady horizontal slope, when calculating TVDI?

A visual inspection and statistical analysis are conducted based on the results of TVDI, to determine which vegetation index delivers better soil moisture estimation. Then, TVDI results are exported to ArcMap 9.3 to classify the results and compare them before and after the illumination correction. Later, the results are compared with the map of wetland of the region. Second, a statistical analysis is implemented by comparing both of the mean value and standard deviation of the vegetation indices (EVI and NDVI) and for TVDI before and after the illumination correction. Then the correlation of the best fit line in both of the dry and wet edge is calculated to determine the changes in correlation before and after applying the illumination correction. Third, pixels' spatial frequency distribution is compared before and after the correction when EVI used and when NDVI is used. Based on the trend of pixels spatial distribution, a comparison is made to evaluate the effectiveness of the estimated results before and after the illumination correction.

4.3.2.1 Visual Analysis

The estimated soil moisture information, represented by the derived TVDI, has been classified a cross the study area, and compared with the map of wetland of the area in the Province of NB. It has been found that the result of TVDI derived from T_s-EVI space

using uncorrected data show inconsistency with some places with the map of wetland. For instance, the TVDI results derived from T_s-EVI using uncorrected data on May 01, 2003 reveal that most of the areas that are located in the northern part of the province of NB are shown wet while they are dry in the map of wetland (see Figures 4.9 (1-a) and (2-a). On the other hand, the estimation results for some areas that are located at the south-eastern portion of the study area are shown as dry while they are correspondent with water body areas in the map of wetland. However, the TVDI results derived from T_s-EVI using corrected data shows more agreement with the map of wetland and does not show this inconsistency. Moreover, the estimated soil moisture around high elevation areas in the north part of the study area was decreased significantly after the data was corrected, and that consents with the map of wet lands and consents with the theory of decreasing soil moisture with increasing topography elevation [Hewlett, 1961; Tamai, 2010]. In addition, the estimation results show that the areas along the coastlines and at some parts of the river channels show higher soil moisture; the estimated soil moisture in the south-east area shows similar results with the results of the wetland map.

A distinct graduation is shown from the dry areas in the southern part to the wet areas in the north for soil moisture distribution when the corrected data is used (see Figures 4.9 (1-b)). Furthermore, the estimation moisture distribution derived from T_s-EVI space using corrected data show better results and more accord with map of wetland compared with the estimation results derived from T_s-NDVI space using corrected data; this better result is clearly seen in the less variation in the estimated soil moisture distribution throughout the study area when EVI is used as compared with the results of using NDVI.

TVDI results derived using NDVI was not successful to detect some water body areas or some disperse vegetation while TVDI derived using EVI was successful to do so (see Figure 4.9 (1-c)).

Similar visual inspections are found in the estimation results when September 30, 2003 dataset are used (see Figures 4.9 (2-a), (2-b), (2-c)). Except that a general observation can be seen in the estimation results of September dataset, which is that disperse water bodies southern the study area are not detected as wet areas unlike the results of using May dataset. However, more areas are shown moist in the northern part of the study area when September dataset is used compared with the results of soil moisture using May dataset and this is in accord with the weather conditions in NB as it is drier in the summer season and wet in the fall season.

Last but not least, when T_s-EVI space is used, it appears that the overall results of soil moisture distribution were relatively better compared with the results of using T_s-NDVI space. The sudden change in the estimated soil moisture around vegetation covered areas was better represented when T_s-EVI space was used rather than using T_s-NDVI space; this better result is shown in the better graduate distribution for soil moisture around the vegetated areas. Soil moisture estimation derived from T_s-EVI space was able to identify the loss of dense forest cover regardless of forest type unlike the result derived from T_s-NDVI space.

Finally, some differences are seen when implementing a visual inspection between the TVDI results derived from T_s-EVI using corrected data and the map of wetland. These

differences are generally shown in the northern part of the study area that shows dry areas in the map of wetland while they are shown as wet in the estimated TVDI map; this differences can be related to the method used to create the map of wetland, which was completely depending on the height difference between water body areas (assumed to have 0 height) and the height of the neighboring areas (their wetness is derived based on the elevation difference between water body areas and these targeted areas) [Research Center at the University of New Brunswick, 2011]. Therefore, the TVDI results are in agreement with identifying the wet areas while at some areas, which have high elevation, they show disagreement.

4.3.2.2 Statistical Analysis

From the drawn T_s-EVI space, the general trend of the pixels located at the wet edge was varying linearly (see Figures 8 (1 and 2)). Therefore, representing these pixels in a linear horizontal line at the scatter plot, as the original method proposes, would not best fit this pixel variation accurately. Thus, the best representation for the pixels' trend is drawn by a linear regression equation that was used as the $T_{s\ min}$ in the TVDI equation.

The T_s-EVI space drawn from the corrected data shows that pixels' distribution in both edges has more coherence and better correlation compared with the pixel correlation at the T_s-EVI space derived from the uncorrected data, (see Figures 4.8 (1-a) and (1-b), (2-a), (2-b), and Tables 2). This better correlation indicates that the pixel values are well

represented in calculating the TVDI equation since the TVDI equation is calculated based on the linear fit equation of each edge in the triangular scatterplot. Furthermore, the σ of the calculated EVI after the data was corrected is lower than the σ for the EVI of the uncorrected data. Similarly for the calculated NDVI that has a lower σ after the data was corrected (see Table 4.3). On the other hand, better correlation among the pixels located at the wet edge and the pixels located at the dry edge has been found when EVI is used compared with the correlation when NDVI is used (see Table 4.2). This better correlation indicates that using EVI in the T_s-EVI space is more effective than using T_s- NDVI space in this particular area.

Lastly, from the perspective of pixels spatial distribution and in general, the TVDI frequency distribution values across the study area confirm the visual and statistical analysis. The graphs show that there is much variation in the frequency distribution of TVDI values before implementing the correction compared with the values distribution after implementing the correction; for instance, in Figure 4.10 (1-b) and (1-c), the number of values that have TVDI=1, which are more dry areas, have dropped from 29000 to 17800 after the correction was applied; this can be interpreted as these areas that had high TVDI values were more effected in solar illumination and reducing the illumination causes the number of illuminated areas to decrease. Similarly for the frequency of values that have TVDI=zero, which are wet areas; these areas were expected to be located in the dark spots of the uncorrected image; after the correction, they have decreased from 27000 to 12000.

Table 4.3 Mean and Standard Deviation of the Data before and after the Illumination Correction

	Before correction		**After correction**		**Dataset date**
Statistical parameter	μ	σ	μ	σ	
EVI	0.276	0.082	0.278	0.077	May 01, 2003
NDVI	0.53	0.162	0.54	0.145	
TVDI from T_s- EVI	0.53	0.39	0.57	0.32	
TVDI from T_s- NDVI	-	-	0.56	0.3	
EVI	0.81	0.216	0.36	0.118	September 30, 2003
NDVI	0.534	0.302	0.59	0.24	
TVDI from T_s- EVI	0.47	0.328	0.47	0.307	
TVDI from T_s- NDVI	-	-	0.43	0.33	

4.4 Conclusion

Although they have been a number of publications propose different approaches to correct the error caused by topographic changes, none of them has evaluated the effectiveness of the proposed illumination-correction approach in most of remote sensing applications including soil moisture estimation.

Here we have used an integrated approach to evaluate the influence of solar illumination error on soil moisture estimation results. Solar illumination problem was reduced from the data based on applying C-correction method and soil moisture information was estimated based on a modified T_s-VI method. The solar-illumination corrected data were employed to estimate soil moisture. From the results analysis, it has been found that reducing the illumination error improved the estimated soil moisture information. The analysis conducted in this study was based on a visual inspection, a statistical analysis and a comparison with the map of wetland of the region. In addition, the modifications made in the structure of the T_s-VI space using illumination-corrected data shows better soil moisture estimation results than using the estimation results using un-corrected data. Particularly, using T_s- EVI space delivered better soil estimation results than using T_s-NDVI space.

Atmospheric correction is not considered in this study as it is assumed to be removed from the data, since MODIS provider claims that the effects of atmospheric gases, aerosols, cloud, and thin cirrus are corrected in the data.

Due to lack of in-situ soil moisture measurements, soil moisture estimation results before and after the illumination correction are classified and compared visually with the regional map of wetland. Therefore, more analysis needs to be implemented to determine the feasibility of classifying the soil moisture information, and the estimation results could be more verified if they were compared with in-situ soil measurements. Further work can also be extended on processing more time series of MODIS data to determine the soil moisture changing over a period of time (years). Finally, testing the approach

with higher spatial resolution imagery may have a potential to deliver more accurate visual and statistical analysis results.

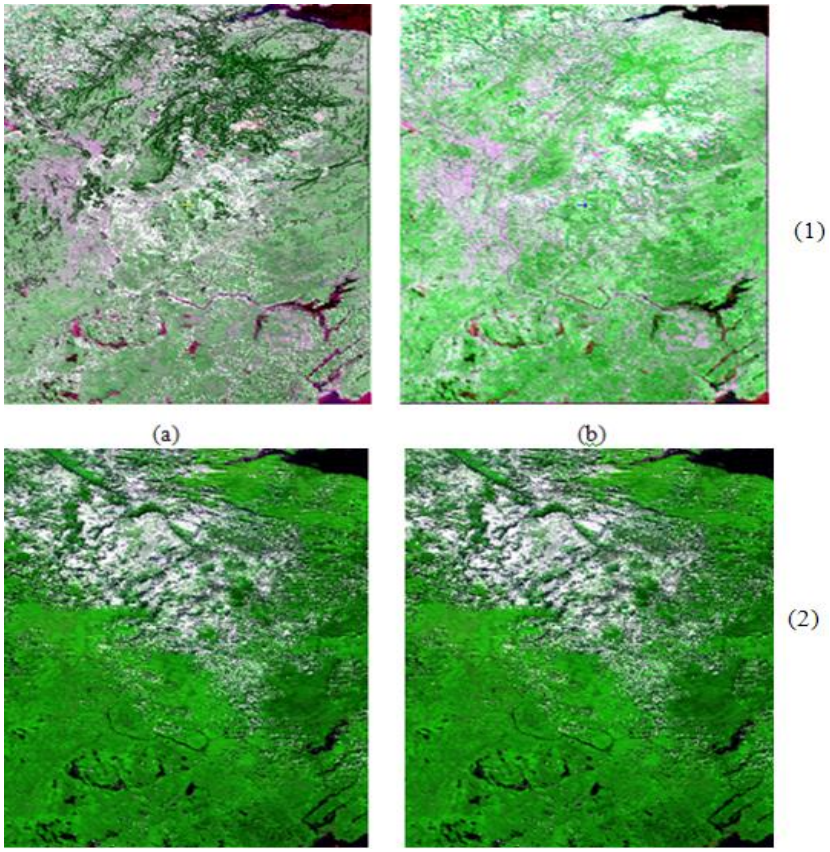

Figure 4.6 MODIS surface reflectance images on (1) May 01, 2003 (2) September 30, 2003.(a) Represents the surface reflectance for bands R, NIR, and B before illumination correction and (b) represents the surface reflectance for R, NIR, and B after illumination correction.

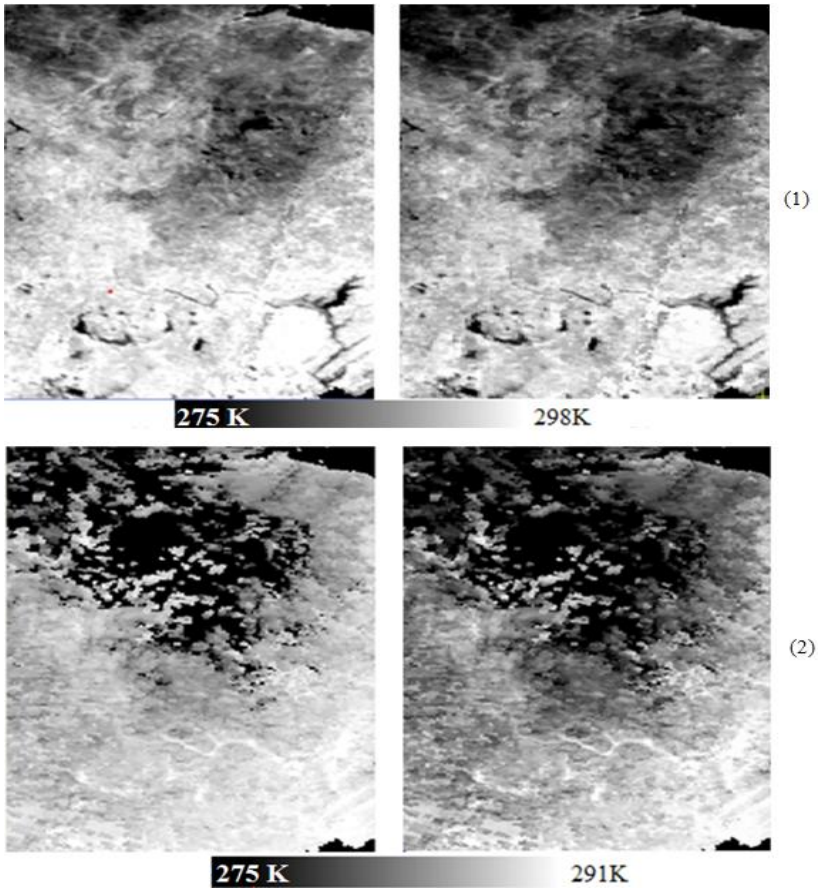

Figure 4.7 MODIS land surface temperature (K) images for (a) May 01, 2003 and (b) September 30, 2003. The left image represents surface temperature before illumination correction; the right image represents surface temperature after illumination correction.

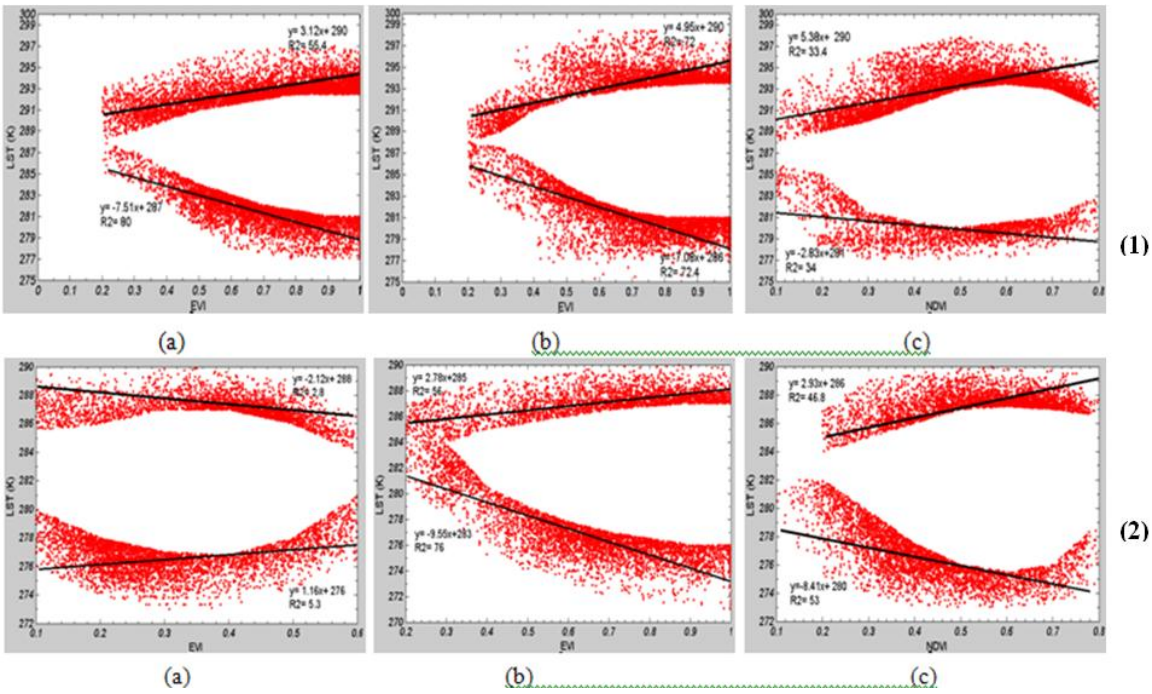

Figure 4.8 Best fit lines for the dry and wet edges (T_{smax} and T_{smin}, respectively) for the T_s-VI space on (1) September30, 2003 and on (2) May 01, 2003; (a) When EVI is used before the illumination correction, (b) when EVI is used after illumination correction, (c) when NDVI is used after illumination correction.

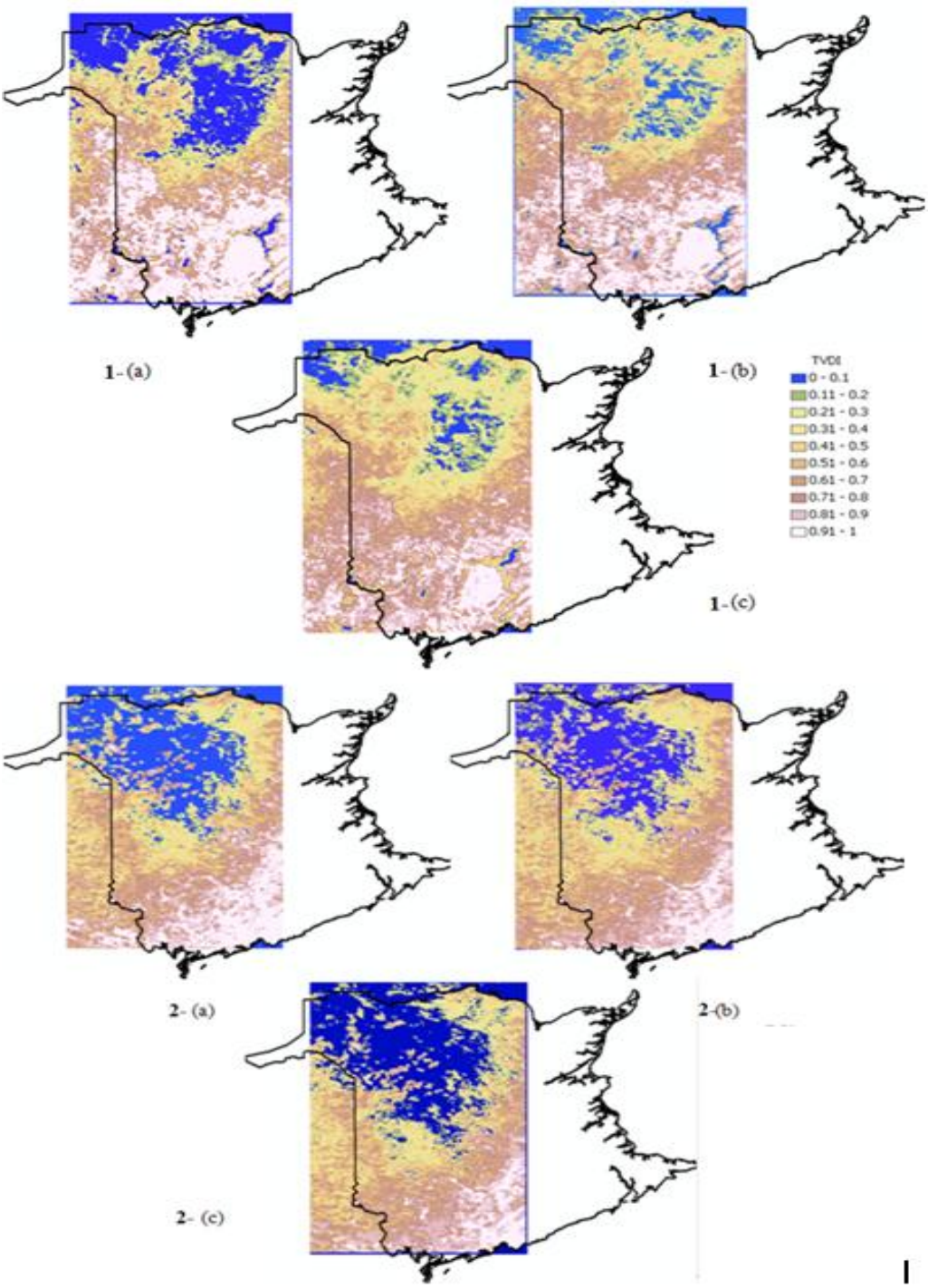

Figure 4.9 TVDI distribution for (1) May 01, 2003 dataset and for (2) September 30, 2003 dataset. TVDI is derived from T_s-EVI space (a) before illumination correction (b) after illumination correction, and (c) from T_s-NDVI space after illumination correction.

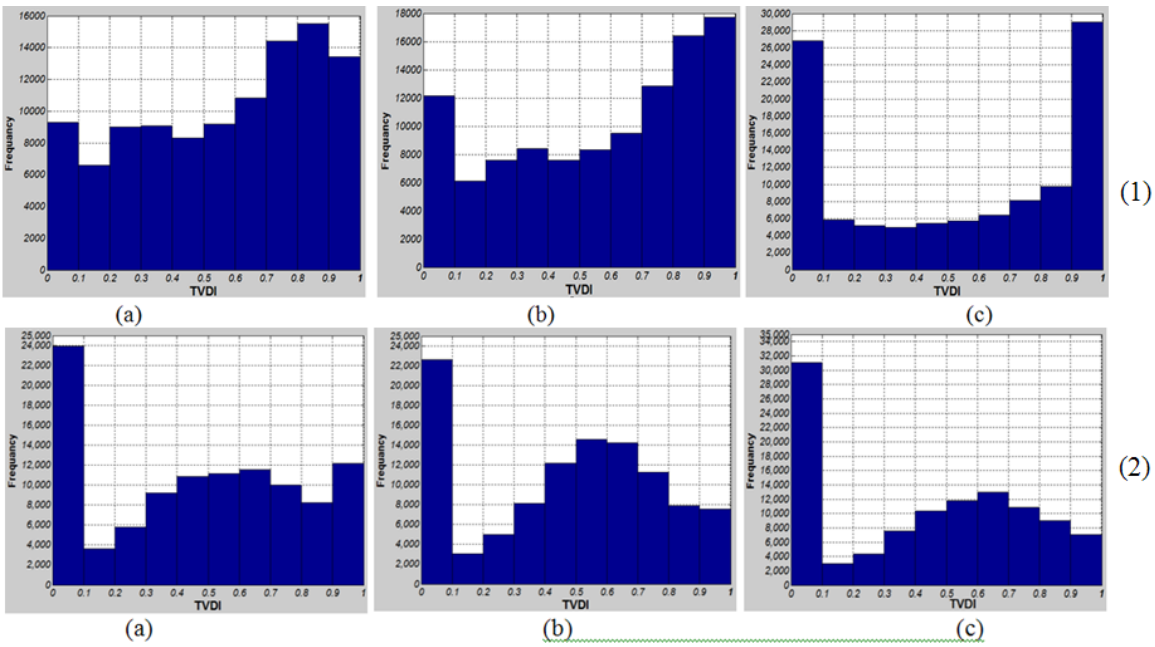

Figure 4.10 TVDI-frequency distribution for (1) May 01, 2003 dataset and for (2) September 20, 2003 dataset. TVDI is derived from (a) EVI before applying illumination correction (b) EVI after applying illumination correction, and (c) NDVI after applying illumination correction.

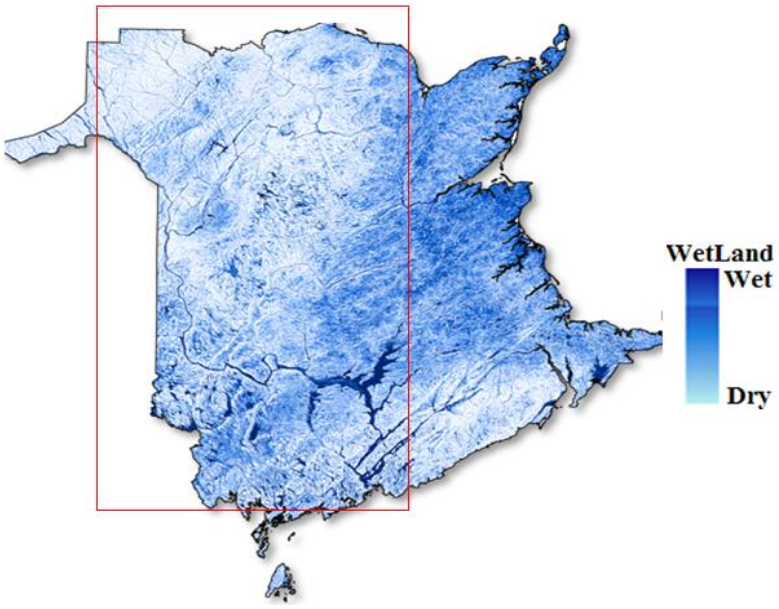

Figure 4.11 Wetland delineation for the province of New Brunswick [Research Centre at the University of New Brunswick, 2011].

Acknowledgment

The author is grateful to Mr. Bahram Salehi, a PhD student at the Department of Geodesy and Geomatics Engineering of the University of New Brunswick, and to Mr. Titus Tienaah, a graduated MSc.E student at the Department of Geodesy and Geomatics Engineering at the University of New Brunswick for their support and feedback concerning the preparation of this manuscript. The author would like to acknowledge the NSERC funding provided by Dr. Zhang, a professor at the Geomatics Engineering department at the University of New Brunswick.

References

Canadian GeoBase data, (2010). Digital elevation data. [online] 5 March 2011. http://www.geobase.ca/geobase/en/browse.do?produit=cded&decoupage=50k&map=021

Carlson, T. (2007). "An overview of the "Triangle Method" for estimating surface evapotranspiration and soil moisture from satellite imagery." *Sensors journal,* Vol.7, pp.1612-1629.

Haibin, L., A. Robock, and M. wild (2007). "Evaluation of intergovernmental panel on climate change fourth assessment soil moisture simulations for the second half of the twentieth century." *Journal of Geophysical Research,* Vol.112, No.D06106, pp.1-15.

Hewlett, J. T., (1961). "Soil moisture as a source of baseflow from steep mountain watersheds." Chapter , U.S. Department of Agriculture-Forest Seroice, Southeastern Forest Experiment Station Asheoilie, North Carolina, U.S., .

Huete, A., K. Didan, T. Miura, E. P. Rodriguez, X. Gao, and L. G. Ferreira (2002). "Overview of the radiometric and biophysical performance of the MODIS vegetation indices." *Remote Sensing of Environment,* Vol.83, pp.195-213.

Itten, K. I., and P. Meyer (1993). "Geometric and radiometric correction of TM data of mountainous forested areas." *IEEE Transactions on Geoscience and Remote Sensing,* Vol.21, No.4, pp.764-770.

Kobayashi, S., and K. Sanga-Ngoie (2009). "A comparative study of radiometric correction methods for optical remote sensing imagery: the IRC vs. other image-based C-correction methods." *International Journal of Remote Sensing,* Vol.30, No.2, pp.285-314.

Kobayashi, S., and K. Sanga-Ngoie (2008). "The integrated radiometric correction of optical remote sensing imageries." *International Journal of Remote Sensing,* Vol.29, No.20, pp.5957-5985.

Law, K. H., and J. Nichol (2004). "Topographic correction for differential illumination effect on Ikonos satellite imagery." *International Arch. Photogrammetry. Remote Sensing Spatial Information Science,* Vol.35, No.3, pp.641-646.

Leprieur, C. E., J. M. Durand, and J. L. Peyron (1988). "Influence of topography on forest reflectance using Landsat thematic mapper and digital terrain data." *Photogrammetric Engineering and Remote Sensing,* Vol.54, pp.1637-1651.

Liu, S., X. Gu, H. Liang, F. Wei, H. Xu, and Y. Dong (2007). "Improved topographic correction approach for radiation of remote sensing image." *SPIE- Interneational Society for Optical Engineering*, Vol.6790, No.1,.

Masek, J., F. Gao, B. Tan, E. Vermote, and R. Wolfe (2010). *"*Traditional illumination correction model*." LEDAPS Update (17).* [on-line] February 1 2011 landsat.usgs.gov/documents/BU_landsat_masek%20copy.ppt

Matsushita, B., W. Yang, J. Chen, Y. Onda, and G. Qiu (2007). "Sensitivity of the enhanced vegetation index (EVI) and normalized difference vegetation index (NDVI) to topographic effects: A case study in high-density Cypress Forest." *Sensors journal*, Vol.7, pp.2636-2651.

McDonald, E. R., X. Wu, P. Caccetta, and N. Campbell (2000). "Illumination correction of Landsat TM data in south east NSW." Proceedings of the Tenth Australasian Remote Sensing and Photogrammetry Conference.

Meyer, P., K. Itten I., T. Kellenberger, S. Sandmeier, and R. Sandmeier (1993). "Radiometric corrections of topographically induced effects on Landsat TM data in an alpine environment." *ISPRS Journal of Photogrammetry and Remote Sensing*, Vol.48, No.4,.

Research center at the University of New Brunswick, (April 2011). New brunswick wet-areas mapping. [online] February 2011. http://watershed.for.unb.ca/NB.

Riaño, D., E. Chuvieco, J. Salas, and I. Aguado (2003). "Assessment of different topographic corrections in landsat-TM data for mapping vegetation types." *IEEE Transactions on Geoscience and remote sensing*, Vol.41, No.5,.

Sandholt, I., K. Rasmussen, and J. Andersen (2002). "A simple interpretation of the surface temperature/ vegetation index space for assessment of surface moisture status." *Remote Sensing of Environment*, Vol.79, pp.213-224.

Sato, Y, and Katsushi I. (1994). "Reflectance analysis under solar illumination.". Research CMU-CS-94-221 by School of Computer Science/ Carnegie Mellon University. Pittsburg, Pennsylvania 15213-3890. http://www.dtic.mil/cgi bin/GetTRDoc?AD=ADA290489&Location=U2&doc=GetTRDoc.pdf

Tamai, K. (2010). "Effects of environmental factors and soil properties on topographic variations of soil respiration." *Biogeosciences journal*, Vol.7, pp.1133-1142.

Tan, B., R. Wolfe, J. Masek, F. Gao, and E. F. Vermote (2010). "An illumination correction algorithm on Landsat-TM data." *IGARSS*, pp.1964-1967.

Teillet, P. M. (1986). "Image correction for radiometric effects in remote sensing." *International Journal of Remote Sensing,* Vol.7, pp.1637-1651.

Thomson, A. G., and C. Jones (1990). "Effects of topography on radiance from upland vegetation in North Wales." *International Journal of Remote Sensing,* Vol.11, pp.829-840.

Twele, A., M. Kappas, J. Lauer, and S. Erasmi (2007). "The effect of stratified topographic correction on land cover classification in tropical mountainous regions," Proceedings of the International Society for Photogrammetry and Remote Sensing (ISPRS) conference.

Wu, X., S. Furby, and J. Wallace (2004). "An approach for terrain illumination correction." The 12th Australian remote sensing and photogrametry conference Proceedings, .

Yang, X., J. J. Wu, P. J. Shi, and F. Yan (2008). "Modified triangle method to estimate soil moisture status with moderate resolution imaging spectoradiometer (MODIS) products." *The International Archives of the Photogrammetry, Remote Sensing and Spatial Information Sciences,* Vol.XXXVII, No.B8.

Zhang, Z., X. Ou, Robert R. De Wulf, F. M. B. Van Coillie, L. P. C. Verbeke, and E. M. De Clercq (2011). "Influence of different topographic correction strategies on mountain vegetation classification accuracy in the Lancang Watershed, China," *journal of Applied Remote Sensing,* Vol. 5, 053512.

CHAPTER 5

CONCLUSIONS AND RECOMMENDATIONS

The presented research in this thesis is an extension of the preceding efforts to improve soil moisture estimation results using optical remote sensing data. The research investigated possible improvements in both the data employed for the estimation process and in the estimation method itself. To achieve the objective of this research, several soil moisture estimation methods that use different remote sensing data were reviewed; the most widely used method was chosen, i.e. the Universal Triangle Relationship Method. Possible modifications that can lead to better soil moisture estimation were applied to the method. As well, the main influential error in the data that affects soil moisture estimation is diagnosed; this error was determined to be solar illumination. Furthermore, the most efficient method to reduce the solar illumination effect was identified and applied.

The research contribution to the body of knowledge, pros and cons of the developed integrated approach, conclusions and recommendations are discussed in section 5.1, 5.2, 5.3and 5.4 respectively.

5.1 Research Contribution

The main contribution of this thesis to the knowledge of the field is represented by the following:

- A literature review on different methods used in remote sensing to estimate soil moisture was conducted. The pros and cons of using each method is summarized; each method is evaluated and then ranked. The review resulted in a peer-reviewed journal paper (Chapter2);
- An investigation is conducted about the challenges and development of the widely used Universal Triangular Relationship Method, which resulted in a conference paper (Chapter3);
- The substantial influence of solar-illumination error on soil moisture estimation is proven through this research. This was concluded based on estimating soil moisture before and after the illumination correction. The research result will be submitted to a peer-reviewed academic journal (Chapter4);
- Modified parameters on the Universal Triangle Relationship Method are used to estimate soil moisture. It was determined that these parameters could deliver better soil estimation results. In contrast, previous efforts have focused on proposing new approaches to correct the illumination effect and have compared the corrected data with the uncorrected data to prove the correction approach's

effectiveness without addressing the correction effect on remote sensing application results; and

- An integrated approach is proposed to reduce the illumination effect in the imagery and the corrected results are employed to estimate the soil moisture information using a modified universal triangle method. The modifications that were applied in the universal triangle method have helped to estimate better results (Chapter 4). This integrated approach, which combines a correction method and an estimation method, will help researchers to investigate both the data improvement aspect as well as improving the methodology's aspect to improve their estimation results, especially in the field of soil moisture estimation. Moreover, this thesis reviewed and compared a wide range of methods that are currently used to estimate soil moisture information from different remote sensing data (Chapter 2).

5.2 Integrated Approach

Integrating an improved estimation methodology for soil moisture estimation and employing rectified data is a unique approach implemented to deliver better soil moisture estimation.

The strength of this approach is that it is implemented based on the most robust existing method to construct the illumination surface, which uses solar azimuth and solar

zenith angles calculated from the same MODIS data rather than uses a theoretical method. However, the drawback of this correction method is that it overcorrects some spots as we observed in Chapter 4. Another limitation is that some data did not improve much after applying the correction; moreover, some spots in the processed data have been overcorrected, which created more of a false correction.

According to Amer et al. [2011], T_s-VI method does not produce the best estimation results, but it is the most widely used method. Therefore, it has been used as a complementary stage in this integrated approach. In this method, drawing the boundaries of the wet and dry edges was done based on the author's judgment of where to locate the pixels that form the wet edge or the dry edge. The estimation results are expected to be different if the drawn boundaries of both edges are different.

Finally, the data source used in this research was obtained from the MODIS-Aqua instrument with a spatial resolution the ranges from 250m to 1km. This low spatial resolution has a considerable affect on the estimation results since a pixel size covers a large area that can vary from wet to dry. Therefore, using high resolution optical remote sensing data could affect the estimation results substantially; T_s-VI method has not yet been tested on active remote sensing data such as LIDAR or LASER data.

5.3 Conclusions

Remote sensing has the potential to replace the in-situ soil moisture measurement. This has not been made possible yet, but continuous research efforts and future

developments in remote sensors and soil estimation methodologies will lead to improvement of the estimation results and gradually replacing in-situ measurements.

From the results analyzed in this research, it has been found that the variation in topography causes solar-illumination to have a substantial impact on soil moisture estimation. Soil moisture estimation has been improved after removing the solar-illumination; further improvement is clearly seen after applying the modified parameters in the triangle method. Another general observation can be drawn from the analyzed results is that more uniform moisture soil moisture estimation values were found for intense vegetated areas and that was interpreted as the estimated value are calculated for the intense vegetation cover not for the bare soil surface under vegetation.

The test area chosen in this research contains different land cover represented by a mixture of water bodies, intense vegetation, and bare soil; in addition to having a high variation in topography. Therefore, testing this approach on an area that has a vegetation cover and variation in topography proved to work effectively.

5.4 Recommendations for Future Work

The proposed approach satisfies the research objective by improving the estimated soil moisture results. Nevertheless, there are a number of possible ways to further verify and refine the results:

- Process more datasets and analyze the estimation results in order to better evaluate the effectiveness of this approach;
- Develop a better technique to identify the dry edge and the wet edge in the T_s-VI method; and
- Investigate other data sources such as a high resolution optical satellite imagery to evaluate the imagery's estimation results.

To complement the presented analysis results of this research, in-situ measurements would have been very helpful to measure the improvement made in the estimation results after the topography variations were removed. Therefore, it is recommended to have in-situ measurements taken at the same time as the processed data to easily validate the estimation results.

Since there was in-situ data measured in both May 2003 and September 2003 across the study area, the initial research's plan was to verify the estimation results with the in-situ measurements as reference data. However, the author was not able to access this data. Therefore, only comparative analysis, represented by statistical and visual analysis, were performed to measure the improvement made after removing the effect of topography changes and after modifying T_s -VI parameters. Further research may attempt to do the following:

1- Set mathematical rules that help identify both the dry and the wet edge in the modified T_s –VI space; and

2- Draw clear assumptions about choosing a suitable VI; for instance, as per Chapter 4's, using EVI delivered better estimation results than using NDVI as EVI is more sensitive to dense vegetation. However, there is no effective measurement to classify the type of vegetation whether it is dense or not.

References

Ahmad, A., Y. Zhang, and S. Nichols (2011). "Review and evaluation of remote sensing methods for soil-moisture estimation." *SPIE Reviews journal,* Vol.2, pp. 028001 1-17.

CURRICULUM VITAE

Candidate's full name: **Amer Abdalla Ahmad**

Universities attended and certificates:

- Al-Mustansiriya University, Sept.1999- Sept. 2003; B.Sc. in Civil Engineering.
- University of New Brunswick, May 2010-Sept. 2010; Diploma in University Teaching.
- University of New Brunswick, Sept. 2010-Sept. 2011; Diploma in Technology Management and Entrepreneurship.

Publications:

Paper 1 (peer reviewed):

Ahmad, A., Y. Zhang, and S. Nichols (2011). "Review and evaluation of remote sensing methods for soil-moisture estimation." *SPIE Reviews journal*, Vol.2, pp. 028001 1-17.

Paper 2:

Ahmad, A., and Y. Zhang (2011). "Development and challenges of applying the Universal Traingle relationship Method in remote sensing applications." Proceedings of the *32nd Canadian Symposium on Remote Sensing and 14th Congress of the AQT*, Sherbrooke, Québec, Canada, June, 13-16, 2011.

Paper 3 (peer reviewed):

Ahmad, A., Y. Zhang, and C. Bourque (2011). "Mapping an Index of Soil-Moisture Using Illumination-Corrected Land Surface Temperature and Enhanced Vegetation Index Generated from MODIS Data." Will be submitted to Remote Sensing of Environment Journal.

Paper 4 (peer reviewed):

Mioc, D., François A., P. Adda, T. Tienaah, A. Ahmad, M. Mezouaghi, E. Mcgillivray, A. Morton, and P. Tang (2011). "Flood progression modeling

and impact analysis." *Proceedings of the International Society for Photogrammetry and Remote Sensing (ISPRS)*, Antalya, Turkey, 3-8 May, 2011.